DESIGN AND TESTING OF LONG-LIFETIME ACTIVE SENSOR ARRAYS FOR IN-CORE MULTI-DIMENSIONAL FLUX MEASUREMENTS

by

TYREL DANIEL FRANK GEORGE

B.S., Fort Hays State University, 2013
B.S., Kansas State University, 2013

A THESIS

submitted in partial fulfillment of the requirements for the degree

MASTER OF SCIENCE

Department of Mechanical and Nuclear Engineering
College of Engineering

KANSAS STATE UNIVERSITY
Manhattan, Kansas

2016

Approved by:

Major Professor
Douglas McGregor

Abstract

Fission chambers are a common type of detector used to determine the neutron flux and power of a nuclear reactor. Due to the limited space and high neutron flux in a reactor core, it is difficult to perform real-time flux measurements with present-day in-core instrumentation. Micro-pocket fission detectors, or MPFDs, are relatively small in size and have low neutron sensitivity while retaining a large neutron to gamma ray discrimination ratio, thereby, allowing them to be used as active neutron flux monitors inside a nuclear reactor core. The micro-pocket fission chamber allows for multiple detectors to be inserted into a flux port or other available openings within the nuclear reactor core. Any material used to construct the MPFD must be rugged and capable of sustaining radiation damage for long periods of time. Each calibrated MPFD provides measurements of the flux for a discrete location. The size of these detectors allows for a spatial map of the flux to be developed, enabling real-time analysis of core burnup, power peaking, and rod shadowing. Small diameter thermocouples can be included with the array to also measure the temperature at each location.

The following document details the research and development of MPFDs for long term use in nuclear power reactors. Previous MPFD designs were improved, miniaturized, and optimized for long term operations in reactor test ports designed for passive measurements of fluence using iron wires. Detector chambers with dimensions of 0.08 in x 0.06 in x 0.04 in were attached to a common cathode and individual anodes to construct an array of the MPFDs. Each array was tested at the Kansas State University TRIGA Mark II nuclear reactor to demonstrate functionality. The linear response in reactor power was measured. These arrays have also demonstrated reactor power tracking by following reactivity changes in steady state operations and reactor pulsing events. Stability testing showed consistent operation at 100 kW for several hours. The MPFDs have been demonstrated to be a viable technology for in-core measurements.

Table of Contents

List of Figures

List of Tables

Acknowledgements

This project was made possible through the support and work done by Dr. Douglas McGregor, Dr. Phil Ugorowski, and Dr. Jeff Geuther. The development of Micro-Pocket Fission Detectors (MPFDs) has been accomplished through the Mechanical and Nuclear Engineering (MNE) Department's Semiconductor Materials and Radiological Technologies (S.M.A.R.T.) Laboratory at Kansas State University (KSU). Testing of the MPFD arrays was completed at the KSU TRIGA Mark-II Nuclear Reactor Facility located in the MNE Department. Undergraduate assistance in the construction and testing of the MPFDs was provided by Hai Vo-Le, Sarah Stevenson, and Daniel Nichols. Additional thanks goes to fellow S.M.A.R.T. Laboratory researchers Benjamin Montag and Ryan Fronk for the helping in the design of the detectors and detector testing. Also, thanks to the nuclear reactor staff for providing reactor time.

The assistance of all these individuals is greatly appreciated.

Dedication

To my parents, Neal and Judy George, for giving the discipline for continuing my education and to my co-advisors Dr. Jeff Geuther and Dr. McGregor for encouraging me to continue my education.

Chapter 1 - Introduction

Various types of detectors are used for measuring the neutron flux of a nuclear reactor to provide information on the thermal power and neutron flux distribution. Neutron Flux distribution maps provide information on the fuel burnup, peak centerline temperature, power distribution, and other characteristics of nuclear reactors. Despite the fact that there are many detectors available for measuring the neutron flux, reactor behavior models still depend heavily on modeling programs, iron wire flux measurements, and other complicated calculations. These computational methods may become inaccurate due to a change in neutron flux over time. Hence, modeling programs do not always replicate the exact environment of the reactor, and iron wire flux measurements are limited to measuring only the overall integrated neutron flux. Therefore, real-time measurements of the neutron flux at different locations are needed to provide accurate neutron flux distribution maps. In this chapter, the basic principles describing real-time measurements and the current state of in-core neutron detectors are discussed. This discussion includes previous design work completed by Semiconductor Materials and Radiological Technologies (S.M.A.R.T.) Laboratory at Kansas State University (KSU) and the motivation for improving these designs.

1.1 Basic Principles

Fission is the process of splitting atoms into lighter nuclei and producing neutrons, energy, gamma rays, and other particles. Nuclear reactors are used as the heat source for electrical power generation, an efficient benefit of the fission process. Reaction products generated from nuclear fission include fission fragments, fast neutrons, gamma rays, neutrinos, delayed neutrons, and charged particles (α and β particles) [1]. These reaction products provide the energy needed to provide the thermal power for the reactor. The recoverable energy from a

single fission is approximately 95%, the 5% loss of energy is a consequence of the low interaction rate of neutrinos [1]. Neutrons released from fission are moderated to thermal energies and can be subsequently absorbed by the uranium-235 fuel to cause more fission. Depending on the number of neutrons absorbed for each generation, the reactor power will be subcritical, critical, or supercritical [1]. A subcritical reactor has fewer fission events each generation, which is manifested as a reduction in reactor power. Critical reactors have the same neutron population for each generation; hence the reactor power is constant. Finally, a supercritical reactor has an increasing neutron population for each generation, resulting in an increase in reactor power. Every reactor core has a unique configuration that determines how each generation of neutrons are distributed through the core. Neutron flux is a quantity used for describing the distribution of neutrons and it is defined as the number of neutrons passing through a unit area per unit time [1]. Neutron fluence is sometimes used to describe the neutron flux integrated over a length of time [1]. Measuring the neutron flux of a nuclear reactor requires the use of detectors that can provide real-time measurements. These measurements are commonly used to provide the reactor power and not information concerning the flux distribution. In a nuclear reactor, neutrons and gamma rays are continuously created from fission events. Neutrons increase linearly with power, thereby, allowing a calibrated detector to measure the power from the neutron and gamma ray flux [1]. However, neutrons have no electrical charge, which complicates their accurate measurement. Detecting neutrons and gamma rays requires using a detection medium that will create secondary particles that can be measured.

Detectors absorb radiation particles and provide a measurable signal associated with each event [2]. Gas-filled chambers are a common type of radiation detectors that use a gas as the

interaction medium for radiation. Radiation absorbed in the gas chamber liberates electrons from the parent nuclei. The free electrons excite additional charges in the gas, thereby, creating a charge cloud of electrons and ions. A signal is provided by placing a voltage across the electrodes of the gas detector and separating these "charge carriers". Separation of the charges induces a current pulse with amplitude that is dependent on the chamber capacitance. At high enough electric fields, impact avalanching can cause charge carrier gain. Typically, a charge sensitive preamplifier is used to convert the induced current into voltage amplitude for readout, defined by $\Delta V=\Delta Q/C$. There are five operating regions of a common gas-filled detector [2]. If a significant number of electrons and ions recombine before the applied voltage separates the ion pairs, the detector is operating in Region I, defined as the recombination region. As the voltage is increased, ion pairs will separate and recombination becomes negligible. Region II starts at the end of the recombination region and is referred to as the ionization chamber region. The applied voltage will separate nearly all of the ion pairs and the total number of electron-ion pairs contributes to the induced signal. Further increasing the applied voltage will allow the detector to operate in the proportional region (region III). In this region, the electrons gain kinetic energy from the electric field and produce more ion pairs through impact ionization [2]. This phenomenon allows for signal gain and is commonly referred to as "gas multiplication". Gas multiplication will increase the current as the applied voltage is increased. The total amount of ionization remains proportional to the energy deposited by the initial radiation particle. Increasing the voltage past region III can cause a gas detector to operate in the Geiger-Müller region (Region IV). Region IV produces excessive gas multiplication, but the space charge accumulation determines the eventual pulse height and not the initial energy deposited or the type of radiation absorbed. Finally, an increase in voltage beyond Region IV causes the detector

to enter region V, the region of continuousness discharge. Detectors can undergo irreversible damage from electrical arching if operated in Region IV [2].

Ionization chamber detectors are commonly used in nuclear reactors to measure neutrons and gamma rays [3]. These chambers operate in the ionization voltage region and do not have charge multiplication [3]. For nuclear reactors, the ion chamber may be designed as a compensated, uncompensated, or a fission chamber device. A compensated ion chamber has two chambers filled with a gas for detecting gamma rays, but one of these chambers is also lined with neutron sensitive material to detect neutrons. The difference in chamber signals provides the neutron generated component [2]. An uncompensated detector has only one chamber containing a detector gas with a neutron sensitive material lining the container. If operated in current mode, the types of radiation depositing energy cannot be distinguished from each other in an uncompensated chamber. Fission chambers are a type of ion chamber, but the neutron sensitive component is a fissionable material such as uranium or thorium (see Figure 1.1).

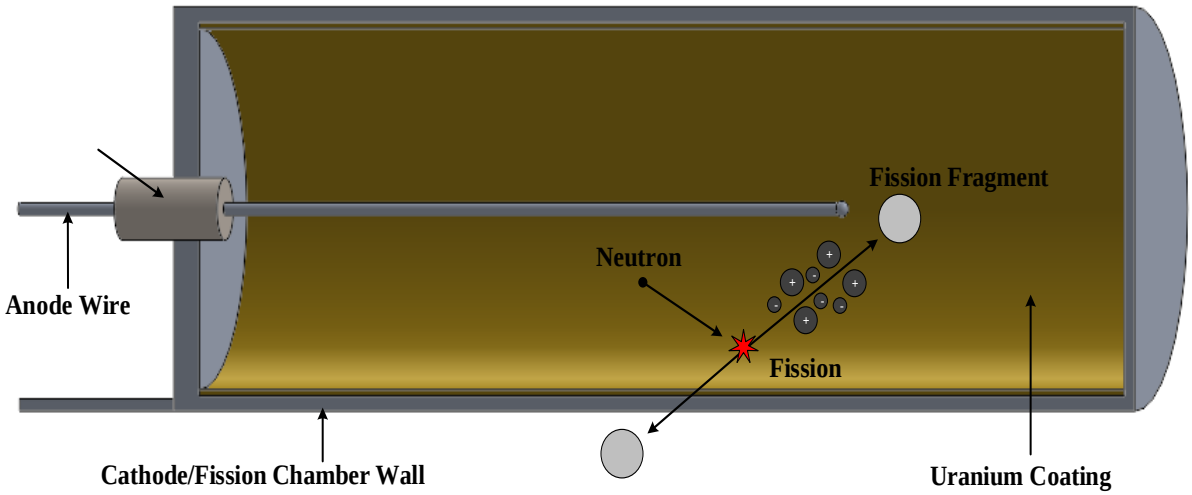

Figure 1.1: The basic design of a fission chamber and the result of absorbing a neutron and causing fission inside the chamber [4].

The detector gas selected for operation should have good electron-ion transport properties and low gamma ray sensitivity. Distinguishing between neutron and gamma radiation can be

achieved with energy deposited. A fission fragment can deposit as much as 50 times the energy of a gamma ray in common fission chambers [2]. The mechanisms for Gamma-ray detection generally require ionization through the photoelectric effect, Compton scattering, or pair production, all of which result in the production of minimum ionizing particles (electrons) that deposit a minute amount of energy in small fission chambers. MPFDs are designed as parallel plate detectors with opposing anodes and cathodes, therefore, providing a uniform electric field for charge separation within the chamber (See Figure 1.1). Neutron conversion coatings often consist of natural uranium or some form of enriched ^{235}U for fission chambers deployed in nuclear reactors. The coating is applied to one or both of the electrodes [4]. As shown in Figure 1.1, a neutron fission site will cause fission fragments to pass through the chamber and deposit energy in the gas. Fission fragments that enter the detector gas will produce electron-ion pairs inside the chamber. These charge carriers can be separated by an applied electric field, the motion of which produces an induced current to flow in the detector circuit, which can also be formed into a voltage pulse.

Ionization and fission detectors can operate in either pulse mode or current mode [2]. Pulse mode allows for the detection of a single interaction event that causes ionization in the chamber [2]. A charging circuit is used to amplify the signal, time-integrate the current, and record the voltage pulse. These voltage pulses represent radiation interaction events and can provide useful information about the radiation field [2]. However, pulse mode is best used for count rates below 10^4 cps, much lower than the expected radiation environment in a nuclear reactor. Detectors operating in pulse mode can suffer pulse pile-up if additional events occur in the detector during the pulse processing time. Pulse pile-up can cause significant detector dead time losses and possibly "paralyze" the detector. Within nuclear reactors, the high radiation field

requires almost all detectors to operate in current mode when operating at high powers. Current mode is used to measure the spontaneous current generated from the radiation induced ionization rate in the detector [2]. The current measured is proportional to the neutron and gamma ray flux and can be used to provide reactor power measurements [2]. Most fission chambers can operate in both modes, but the detector will be switched from pulse mode to current mode when dead time causes the count rate to deviate from linearity [5].

1.2 Extant Fission Chambers

Commercial fission chambers are separated into two categories, depending on the location that the detector will be deployed with respect to the reactor core. "Near-core" detectors are placed outside of the fuel lattice structure, and most near-core detectors are placed between the graphite reflector and the reactor containment vessel [6]. "In-core" detectors are generally placed within the actual reactor core, often within vacant fuel spacing or the narrow coolant channels available in the fuel lattice structure [7, 8]. The detectors described below have different properties, depending mainly on the fissionable material, inert gas, and size of the detector. Neutron reactive coatings for fission chambers range from a few micrograms to several milligrams [7]. The efficiency and sensitivity are controlled by the thickness of the coating, surface area covered, and the fission cross section [8].

Near-core detectors include any detector that must remain outside of the reactor core and graphite reflector (if present) to prevent extreme dead times and radiation damage. Due to the lower neutron flux, detector life-times are usually longer than in-core detectors and the detector is prevented from causing flux perturbations [6]. Often near-core detectors have several milligrams of ^{235}U to achieve a high sensitivity to measure the flux [5]. Also, the relatively large amount of uranium is used to provide a signal at low powers of 10 W or less [6]. Similar

detectors can be used for beam port calibrations, but require several grams of ^{235}U [8]. The design of near-core detectors depend on neutrons leaking from the reactor core and do not provide a true representation of the flux distribution. Because of the lack of size restrictions, most near-core detectors are large, simple designs similar to that shown in Figure 1.1 [6]. None of the detectors are designed to be moved after being calibrated and are constructed of materials that become extremely radioactive after exposure [8]. Therefore, relocating calibrated detectors to various points outside of the reactor core is impractical and provides almost no information on the neutron flux distribution of the core. The properties listed above for near-core detectors prevent them being used for mapping the reactor neutron flux and also from being removed from the core without extensive shielding and appropriate safety protocol.

In-core detectors are designed to withstand high temperatures, pressures, and radiation fields. Most detectors have a diameter on the order of 10 mm and length of 10 cm (or greater) [7]. The detector size allows for insertion into the coolant channels at most electrical power nuclear reactor cores. Smaller in-core detectors have less neutron reactive material, on the order of a few micrograms of ^{235}U coated inside the detector, thereby preventing significant flux perturbations [9, 10]. These detectors can provide real-time neutron flux mapping in various locations of the reactor core. However, coaxial detectors of such small size are difficult to produce and can be expensive. Neutron flux measurements are a function of detector length, which also affects the spatial resolution of the axial flux. Another disadvantage is that long term usages with these devices are impractical due to the gradual burn-up of the neutron-sensitive material and also catastrophic radiation damage [6, 11]. In-core detectors are constructed of materials that produce radioactive isotopes with extremely long half-lives. Very few of these available detectors are built with materials that are insensitive to neutron activation or have short

radioactive half-lives. Further, these commercial fission detectors are not designed for specific nuclear reactor cores, and cannot be changed for unique differences in reactor cores [10]. Finally, commercial in-core detectors cannot be deployed within the flux wire ports often available between fuel elements. Flux wire ports are designed for iron wire calibrations and have diameters less than 5 mm [12, 13]. Smaller fission chambers that can be deployed within small locations in a reactor core have been studied and developed at KSU.

1.3 Previous Design Work

Micro-pocket fission detectors (MPFDs) are fission chambers designed for deployment in smaller spaces within a nuclear reactor. At KSU, the S.M.A.R.T. Lab has developed fission chamber detectors with widths of 2 mm or less [12, 13]. As shown in Figure 1.2, the MPFD design is a parallel plate with a fissionable material coating on one plate. Each MPFD node consisted of three detectors that measure the fast flux using ^{232}Th, thermal flux using ^{235}U, and the background using no fissionable material [12-15]. Each array consisted of four sets of MPFDs that can be positioned evenly over the active fuel region of a nuclear reactor [16]. These arrays were tested at KSU's TRIGA Mark-II nuclear reactor using the flux ports located between the fuel elements. The arrays demonstrated linear operation capabilities from reactor shutdown up to 200 kW [16]. Results of the linear operation also showed that at full power the observed count rate suffers 24% dead time [13]. Stability tests showed that the detectors could consistently operate after receiving neutron fluence greater than $6 \times 10^{16}\ n/cm^2$ [13]. Similar results show that the materials used in assembling these detectors can withstand the high radiation fields seen at even a nuclear power reactor [15-17].

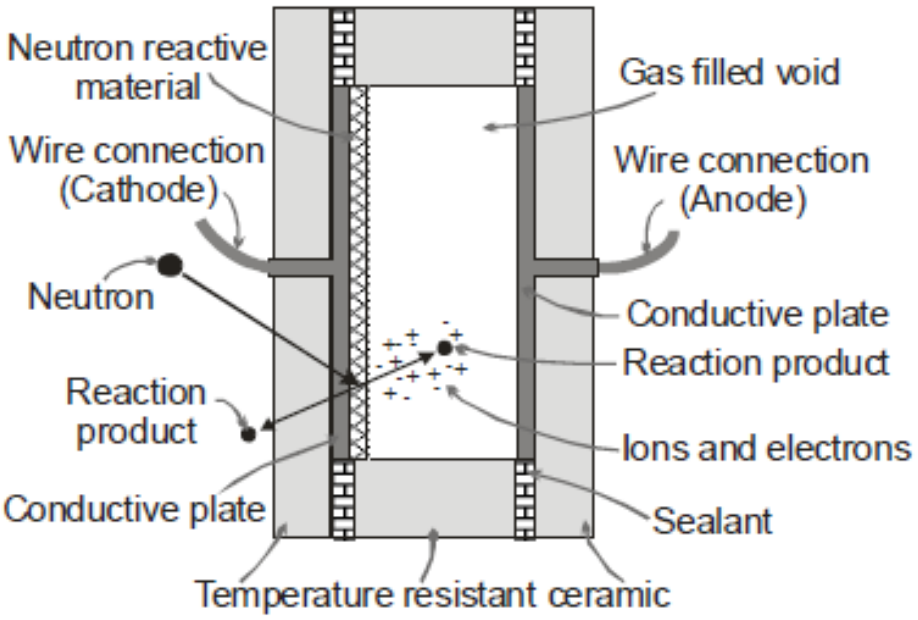

Figure 1.2: The cross-sectional view of the first MPFDs developed at KSU and a neutron induced fission ionizing the gas in the chamber [12, 17].

MPFDs reported in the literature [12-15] were significantly smaller than traditional fission chambers, thereby, enabling deployment in tiny locations within the reactor core. Previous work included multi-node MPFDs capable of several simultaneous neutron flux measurements along a single axial location. It also provided a basis for determining the spatial count rate resolution of a detector array for in-core measurements. The MPFD design shown in Figure 1.2 provides a general foundation for the continuation of MPFD research at KSU and for this thesis. However, the MPFD arrays of prior work were large enough in diameter such that the flux port locations needed to be expanded from 4 mm to 8 mm diameters. MPFDs were installed into these retooled flux ports, but the MPFD design did not offer flexible detector arrays that can be deployed in the flux ports of standard research nuclear reactors. Improvements were needed such that MPFDs can be inserted into smaller flux wire ports (see Figure 1.3). One such improved device, designed by KSU for Idaho National Laboratories (INL), is shown in Figure 1.3.

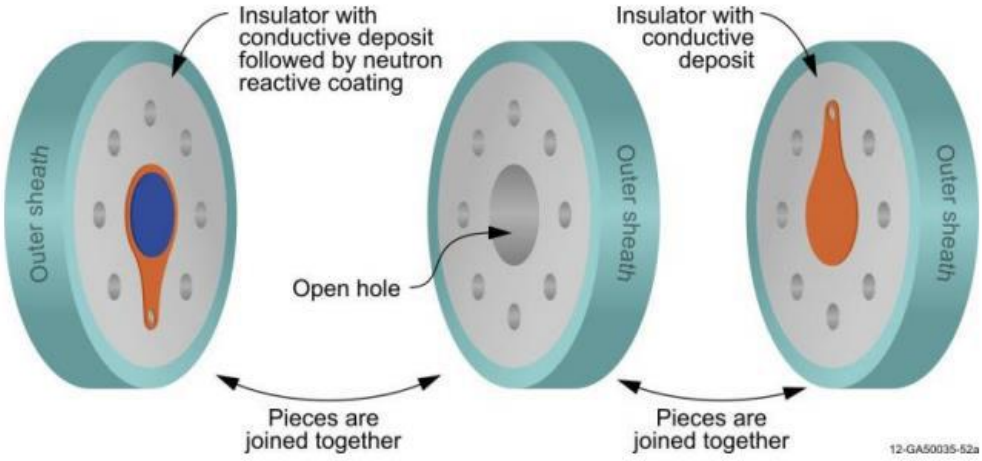

Figure 1.3: A redesigned MPFD chamber used for possible multi-node arrays developed for INL [18].

The MPFD design of Figure 1.3 was developed for INL as a dual chamber MPFD array to measure the fast and thermal flux. Both MPFD chambers have a diameter of 2 mm and height of 1.5 mm [18]. One chamber was electroplated with natural uranium and the other was electroplated with thorium [18]. This array was tested at the KSU TRIGA Mark II nuclear reactor and it successfully demonstrated as an in-core neutron sensor. Designs similar to Figure 1.3 were used for early generation MPFD detectors and also provide the motivation for the present work.

1.4 Motivation for Redesigning MPFDs

Organizations in the nuclear industry have shown an interest in using multi-node MPFD arrays to determine the axial flux at various locations with a high degree of spatial resolution over extended periods of time. A neutron flux map of a nuclear reactor can provide real-time fuel burnup and power distribution information for researchers so as to design better reactors and also lead to increased understanding as to how fuel loading changes the core performance. Motivation for this project includes the need for detector arrays designed to be durable and flexible enough to insert into compact locations within a multitude of nuclear reactor designs. It

is also required that custom detector arrays be available at a reasonable price. Nuclear reactors such as KSU's TRIGA Mark-II have expensive fission chambers that are not designed for in-core testing and are designed to operate in a specific configuration. Understanding reactor behavior involves using intensive applications of simulation programs, flux measurements, and in-depth calculations. Despite all of the effort spent on understanding reactor performance; the calculated flux distribution of the TRIGA MKII nuclear reactor still has a sizable margin of error. This error is due to the fact that simulations do not always replicate the exact reactor environment, flux measurements are sometimes not real-time or reliable, and calculations are often simplified to arrive at an answer. Described in this thesis is an attempt to further develop MPFDs for utilization as long term measuring devices of a nuclear reactor flux at any core location. The detector development includes maximizing the number of nodes in a detector array that allow for insertion into various nuclear reactor designs. These MPFDs will also have thermocouples attached at selected nodes in order to measure the local core temperature. MPFD arrays must be able to measure the thermal flux range expected in a pressurized water reactor (PWR) while withstanding the high temperature of a PWR. Finally, the detectors should seek to maximize operational lifetime in a PWR neutron flux while limiting the isotope inventory produced in the detector.

Chapter 2 - Micro-Pocket Fission Detector: Design Considerations

Design changes made to the previous MPFD work focus on developing smaller chamber sizes, extending the detector lifetime, and inserting the detector array into flux wire ports. Motivation for the project and all of the design considerations will determine the extent of the design changes. In-core neutron testing and mechanical failure testing (mock-up testing) will establish the limitations of the final design. This chapter will focus on the project constraints and the desired characteristics of the final MPFD array. Characteristics of the array will include the material analysis and the design structures of the MPFD array.

2.1 Project Constraints

Previous MPFD work demonstrated neutron sensitivity and the possibility of developing smaller fission chambers. The present design constraints for a small, long-term MPFD array require the maximum allowable nodes for insertion into flux wire ports with diameters smaller than 3 mm. Each array will contain a central, common cathode and individual anode wires for the detectors. At least two thermocouples will be included with the MPFD array to measure the temperature. Any material included in the assembly will have the following properties: neutron transparent, resistant to radiation damage, resistant to high temperatures, and low isotope inventory. Lowering the isotope inventory will minimize the mass of long lived radioactive isotopes which will reduce after reactor shutdown dose. This will also be achieved by using high purity material with small neutron absorption and short radioactive half-life. To reduce the isotope inventory, all weld joints will be removed from the designs and mechanical terminations will prevent failure from radiation damage. Other constraints for the MPFD array include using flexible material that still provides structural integrity for inserting and removing the array from a flux wire port. Removal of the array will require the combined strength of all the wire to

exceed 100 lbs. or have a tensile strength greater than 30,000 psi. After removal from the flux wire port, the array will leave minimal material behind to prevent the contamination of the port. All design constraints will require a large cathode wire for structural strength, small anode wires for flexibility, neutron transparent material for low activation rates, and materials that are resistant to radiation damage.

2.2 Material Analysis

Described in this section are the materials suitable for long term deployment inside nuclear reactors. Common materials used inside reactors include nickel alloys, zirconium alloys, aluminum alloys, and ceramic materials. Ceramics provide excellent radiation damage-resistive material and are widely used in nuclear reactors. Materials suitable for nuclear reactors will be used for the wire insulation, the MPFD chamber, the detector wire, and the thermocouple wire. A type of shrink tubing is discussed for implementation in testing due to the physical properties of the material. All the materials used for assembling the MPFD array are based on general by-product calculations that were developed for neutron activation analysis and isotope generation (see Appendix A). All by-products calculated in this section will be for one gram of the material irradiated at 500 kW for one hour. By-product calculations for a single material will provide the initial dose rate after shut down and the dose rate after a month. Dose rates will be provided in units of Rad/hr to provide a measurement of the energy absorbed by the body, but not as a measure of the relative biological effect to the body. The materials that are of interest have one or a combination of low activation, long half-lives (greater than a month), or short half-lives (less than a month). As discussed below, all of the materials are heavily utilized at nuclear reactors and reliable data is available for the radiation damage caused over long periods of time. Finally, reactor workers often process similar radioactive waste and will know how to dispose of the

MPFD array. The materials used in constructing the array are discussed in the following sections. Components of the array include the detector wires, thermocouple wires, insulation, and the MPFD substrates.

2.2.1 Wire Insulators and MPFD

During the research into wire insulators, the only material available for long term in-core insulation was 99.8% pure alumina. Alumina withstands high radiation fields in nuclear reactors and radiation damage sites will not cause material fracturing [19]. Also, alumina has low activation rates and isotopes decay within several minutes. By-product calculations show that 99.8% pure alumina has an initial dose rate of 177.5 R/hr and after one month the dose rate is not measurable (see Appendix A). Ceramic materials also have melting points ranging from 1800° F to 3000° F and can handle the common temperatures of a PWR (600° F) [19, 20]. Various types of plastic insulators can withstand the high temperature of a PWR, but will suffer crippling damage from the radiation [20]. As expected, any plastic material will suffer catastrophic damage and lose its insulating properties. Also, degrading plastics leave material in the flux wire port when removed from the reactor core. Therefore, materials with low neutron cross sections and high temperature melting points are the preferred material. Other materials were investigated for use in a nuclear reactor; such as, silica and magnesium oxide. These materials are preferred over alumina due to the flexibility. Long strands of alumina insulator cannot bend, resulting in reduced flexibility. Unfortunately, the technology to provide small diameter silica or magnesium oxide insulator is still being investigated. Future iterations of this detector could be improved by using these materials when the technology becomes available. To provide flexibility for insertion into flux wire ports, alumina can be cut into smaller pieces to provide insulation over the wire. The selection of MPFD chamber substrate material involved the

analysis of the material properties against similar criteria, and also resulted in alumina being demonstrated as a suitable material. Alumina has high compressive strength and allows for designing fission chambers similar to Figure 1.3 [19]. Alumina substrates can have various sizes of holes drilled through it for wire insertion or chamber spacing. Therefore, the detector components and wire insulator will use 99.8% pure alumina.

2.2.2 Detector and Thermocouple Wire

Electrical wires used to attach the MPFDs provide the structural integrity of the array during the insertion and removal from the flux wire port. Anode wires must be extremely small and the cathode wire must be slightly larger to add structural integrity. A thicker cathode wire will allow the detector to be removed from flux iron wire port without leaving anything behind. Different wire sizes require the material chosen to have available wire gauges smaller than the 3 mm diameter flux wire tube. The type of anode and cathode wire material will determine if the design constraints are met. To meet the structural integrity specifications, the must have a high tensile strength and low radiation brittleness to enable detector removal. Brittle wires can break during the removal of the MPFD array and leave parts of the assembly behind. Several papers provide information on the metal brittleness due to radiation hardening [21, 22]. Wire materials studied in this section are evaluated using linearly extrapolated data from similar materials in the papers [21, 22]. Inconel is a nickel alloy used in the construction of PWRs and has reliable, well-known radiation hardening properties. Nickel alloys are durable and have high tensile strength. Also, alloys such as chromel c are commonly provided in small wire diameters. Table 1 has the non-irradiated tensile strength, irradiated tensile strength, and equivalent displacements per atom (DPA) of three Inconel alloys. DPA is the number of times an atom is displaced for a given fluence [21, 22]. For example, 316 stainless steel will have 4 DPA at 1 MW/m^2 (4.43x10^{13}

$n \cdot cm^{-2} \cdot s^{-1}$) for a single full power year [21, 22]. The amount of radiation damage that a material receives can be determined by measuring the reduced tensile strength after receiving a known dose.

Table 2.1 Initial Tensile strength and irradiated tensile strength after 10 DPA of radiation damage for Inconel 600, Inconel 718, and chromel c [21, 22].

Radiation Hardening Analysis					
Material	Nickel Conc. (%)	Initial T.S. (ksi)	Dose Rate (DPA)	Final T.S. (ksi)	T.S. Reduction (%)
Inconel 600	51.0	120	10	103	13.50
Chromel C	60.0	100	10	86	13.65
Inconel 718	72.0	210	10	181	13.80

Data provided in Table 1 is for precipitation hardened Inconel 600 and solution-annealed Inconel 718. Also, the two metals are used to demonstrate viability of chromel c wire (see Table 1). Chromel c has a composition that is between the two Inconel alloys. Therefore, a linear extrapolation was taken from between Inconel 600 and 718 to determine the reduction in the tensile strength of chromel c wire. Calculations for the chromel c wire in Table 1 shows that the wire will retain over 86% of the tensile strength over the detector lifetime. A dose rate of 10 DPA is used for the data in Table 2.1 to match the full power year of a PWR for five years.

Similar tensile strength analyses were applied to aluminum and tungsten. All of these materials show an increase in brittleness due to radiation damage, but the materials would survive during removal of the detectors. Despite low radiation damage effects, the materials failed other design constraints. By-product calculations show that tungsten has an initial dose rate of 43.5 Rad/hr and after one month a dose rate of 0.0127 Rad/hr. Dose rates show that ^{187}W isotopes quickly decay away, but ^{185}W has half-life of 74.8 days [23, 24]. This means that

several grams of tungsten will result in a significant dose and require several months to decay away. For the mechanical properties, tungsten has a tensile strength of 100 ksi, but tungsten is a hard metal resulting in plastic deformation during the mock-up test. Similarly, aluminum has an initial dose rate of 253 R/hr, but all the isotopes are short-lived. After one hour, the dose rate is 0 R/hr and completely safe to handle. Despite low activation, aluminum wire is not available in small wire diameters and the 11,000 psi tensile strength is less than the required 30,000 psi [25]. Therefore, the material selected for the anode and cathode wire was chromel c high-temperature nickel wire [25]. The composition, physical properties, and available wire diameters of chromel c meet the design considerations of the new MPFD arrays. Analysis shows that the wire will retain over 80% of the initial tensile strength after irradiation for five years in a PWR. Also, the initial dose rate of one gram is 0.131 Rad/hr and after one month the dose rate is 0.056 mRad/hr.

Similar analysis of the thermocouples was performed to determine the dose rate and tensile strength of the wire. Nuclear reactors commonly use K-type thermocouples, which are useful for measuring temperatures up to 2250° F in non-oxidizing or inert atmospheres [26]. K-type thermocouples wires are chromel and alumel. A by-product calculation for the chromel wire dose rate provides the same results as the wire used for the anodes and cathode. Alumel has a 5 Rad/hr initial dose rate and after one month the dose rate was 5 mRad/hr. For the tensile strength analysis, both metals are nickel alloys and have a similar composition to the chromel c wire used for the anode and cathode. Therefore, values from Table 1 for the percent reduction in the tensile strength of the irradiated chromel c wire are used for both thermocouple wires. Chromel thermocouple wire has the same tensile strength as chromel c (100,000 psi), but alumel only has a tensile strength of 48,000 psi. Thermocouple wire used in the MPFD assembly will have smaller diameters than the anode and cathode wires. The small diameter and radiation

hardening will increase the chance of wires breaking during the removal of the MPFD array from a flux port tube. However, the wires will be held together with ceramic insulator allowing for most of the force to be exerted on the chromel wire. Due to these design considerations, the thermocouples will consist of alumel and chromel wires.

2.2.3 Polytetrafluoroethylene (PTFE) Shrink Tube

All of the materials discussed up to this section are used to build a functioning, long-term detector. Other materials were studied to provide assistance with controlling the mechanical properties of the array during the insertion process. PTFE shrink tube provides a lower coefficient of friction between the MPFD array and the tube wall than alumina. This will increase the number of detector nodes on a single array and prevent damage from the insertion process. Properties of the PTFE include: insulating capabilities, low coefficient of friction, and high melting temperatures [27]. However, the radiation damage to the PTFE will prevent any properties from lasting very long in a nuclear reactor [27]. PTFE fluorocarbons are destroyed in high radiation fields which result in carbon and fluorine dust. If PTFE is added to the MPFD array, only the material in the active flux region of a reactor will disintegrate. Most importantly, the PTFE will not affect the functionality or the behavior of the MPFD detectors. The main goal of the shrink tube is to lower the coefficient of friction for insertion into flux wire ports and prevent damage while the array is inserted. Insulating properties of the detectors will still depend on the alumina insulator, but the PTFE will assist it in low radiation areas above the reactor core. Material analysis of the PTFE shows that the carbon and fluorine isotopes have short half-lives and will be gone within a day after shutdown of the reactor [28]. Therefore any PTFE dust left inside or removed with the detector at end of life will decay away quickly and have no harmful effects. PTFE dust left in the reactor core is undesirable due to the possibility

of the dust causing detector interference and electrical shorts. Therefore, the PTFE will not be used in the detector region of the array. The PTFE will enclose the MPFD assembly from the top of the array to a foot above the first MPFD detector. This prevents the neutron flux from damaging the PTFE past the point of failure.

2.3 MPFD Structure

There at two limiting factors for maximizing the number of MPFDs on a single array. The first limitation is the size of the MPFD chamber. Secondly, the diameter of the flux wire tube will determine the maximum number of anodes that can pass by the top MPFD. Reduction and development of the initial MPFD design is the main focus of this section. In this section, previous MPFD designs provided by S.M.A.R.T. Laboratory will be redesigned to provide a final fission chamber that will help maximize the number of nodes on a MPFD array for use in flux wire ports with a diameter less than 3 mm.

2.3.1 Original MPFD Design

Previous MPFDs developed for in-core testing have diameters of 2 mm and are limited to 6 mm diameter tubes (see Figure 1.3) [17, 18]. The MPFDs can be inserted into a 3 mm flux wire tube, but other detector wires passing the top detector will have very little space. Also, the bulky design of the MPFD array will cause damage to the insulated wires during the insertion process. Preventing damage to the insulated wires will require a new MPFD design that will safely allow the anode wires to pass by the detector. Modifying the MPFD chambers in Figure 1.2 and 1.3 provided the first design iteration that would allow the anode and thermocouple wires to safely pass by the chamber. The design is shown in Figure 2.1 and will further be redesigned to determine the maximum number of MPFDs and the limitations of the detector chamber.

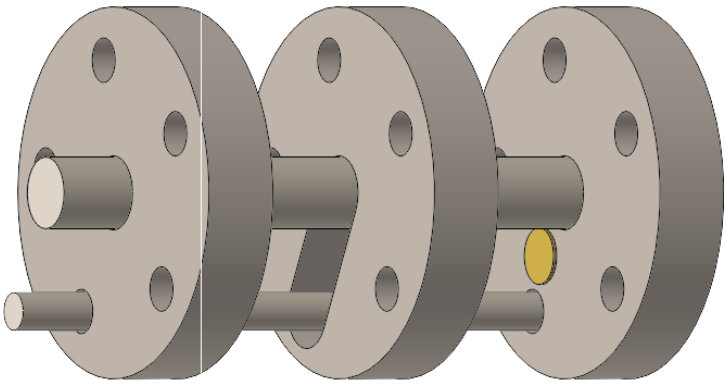

Figure 2.1: The first MPFD design iteration for increasing the number detectors and safely allowing the wires to pass through the chamber region without being damaged.

Spacers have a small region that will allow for fission fragments to pass through and deposit energy. One disk will contain the electrodeposited ^{235}U for thermal flux measurements and the other disk will have electrodeposited ^{232}Th to improve detector lifetimes. Thorium improves the detector lifetime by absorbing a neutron and beta decaying into ^{233}Pa which subsequently beta decays into ^{233}U [23, 24]. Uranium made by the thorium through breeding is created at a rate that matches the loss of uranium from the other disk. This process allows the detector lifetime to be controlled by the amount of uranium and thorium added to the disks. Figure 2.1 also allows for the number of detectors to be increased depending on the ability to machine alumina. The maximum number of detectors depend how many anode holes can be drilled into the substrate without causing structural weakness. For the design in Figure 2.1, the MPFD array is limited to five detectors.

2.3.2 Final MPFD Design

All previous MPFD designs to date prevent the maximum number of five detectors from increasing without sacrificing thermocouples. Therefore, the original MPFD design was reduced in size to accommodate more detectors. The disks in Figure 2.1 have been reduced by removing

the alumina wire holes for the anodes not passing through the detector. Leaving only a cathode and one anode wire hole allows for the alumina substrates to be reduced in size. Only the material surrounding the fission chamber needs to remain, as shown in Figure 2.2. There is room for the cathode and anode wire to travel the full length of the MPFD and terminate on the other side. A spacer holds the two disks apart providing the defined area of the chamber. Also, the spacer has a small section removed from the wall to allow for gas to flow through the chamber (see Figure 2.2). The gap allows for the entire flux wire port to be purged with an ionization gas rather than just around the detector chamber. A sealed flux port filled with the ionizing gas will continuously flow through the fission chambers and replenish the used gas.

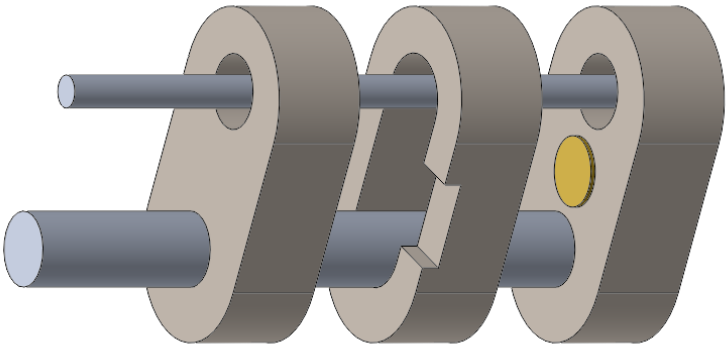

Figure 2.2: The final redesigned MPFD used for assembling and testing the MPFD arrays at KSU.

The final MPFD design has several new features that make the detector superior to the previous design iterations. First, the cathode and anode wire can be terminated after the fission chamber and the termination sites can be mechanical. Mechanical termination does not require adhesive or wire bonding methods, which are weakened by radiation damage and will activate, thereby, increasing the dose rate during removal. Another important feature of the design is the limitation of the MPFD size. Previous designs were limited by the size of the disk and the chamber used to keep the detector pressurized with ionization gas. Sizes of the new detector

design are limited by the manufacturing capabilities of the alumina substrate, cathode/anode wire, and electrodeposited fission material. Finally, the MPFD design will allow for the fission chamber to increase axially without reduction in the electric field and allow for fission fragments to deposit more energy.

2.4 MPFD Array Design

The first MPFD array design iteration is based on the MPFD chamber in Figure 2.1. Structural integrity of the array and the detector spacing relied on using a spring. A spring allows for the array to be pushed up and down while providing compression indicating when the bottom of the tube is reached. Manufacturing these springs with diameters smaller than 3 mm but several centimeters long proved infeasible. Therefore, the design of the array was changed to utilize the alumina insulator to provide the structural integrity and detector spacing. To provide the structural integrity, several types of insulators are used depending on the number of MPFDs. McDanel Advanced Ceramic Technologies provide one- and four-hole insulators for wire gauges as large as 36 American Wire Gauge (AWG). Available sizes of the insulator determined the wire sizes to be the following: 36 AWG (0.127 mm) thermocouple wire, 34 AWG (0.160 mm) anode wire, and 26 AWG (0.405 mm) cathode wire. Figure 2.3 shows the single-hole and multi-hole insulators used for each wire type [29]. Also, larger wire diameters are available for the insulators shown below, but the tolerances of the alumina insulator may prevent the insertion of the wire. Four-hole insulators are large enough to allow the four wires to change to single-hole insulators without leaving a wire gap at the transition site. In order to replace the spring design, the alumina insulator has to be broken into multiple pieces to keep the flexibility and provide the structural stability to insert the array into the flux wire port. Structural integrity of the array is improved as the maximum number of MPFDs is reached.

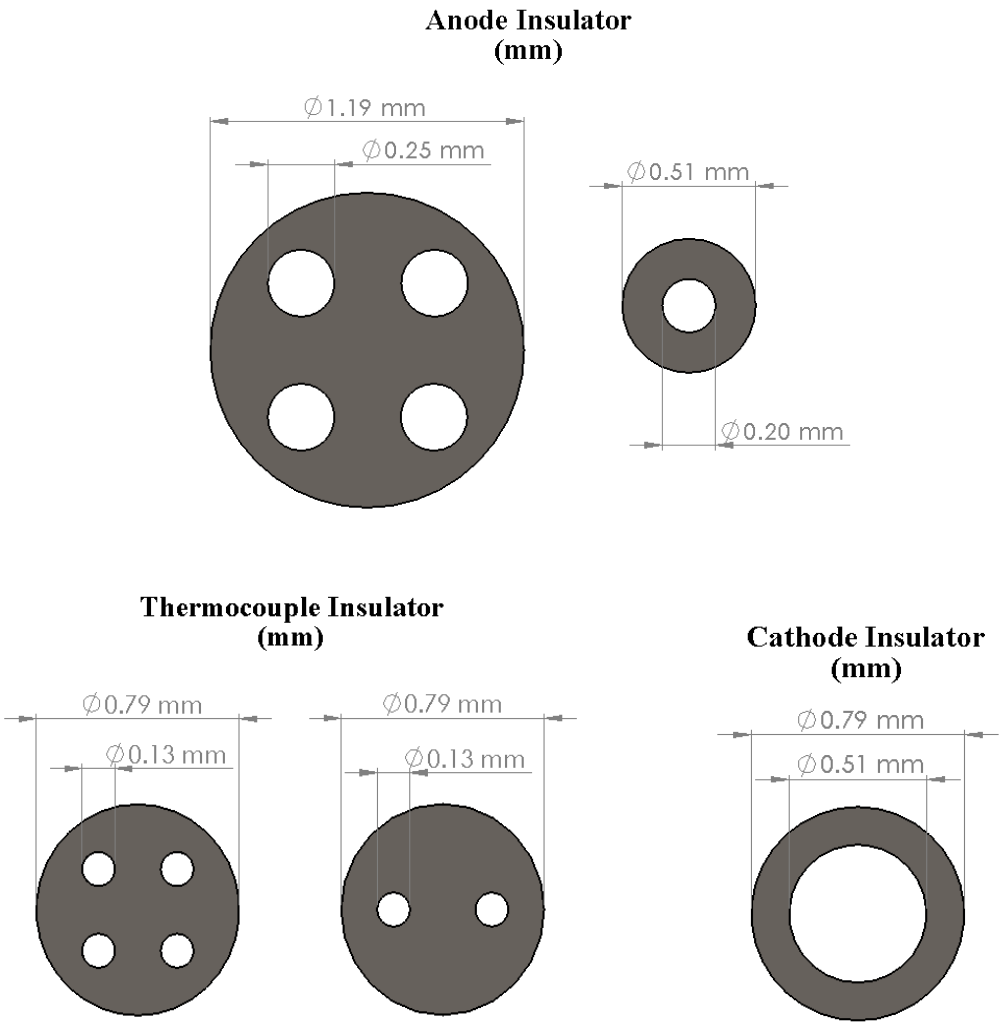

Figure 2.3: (top) Size measurements of the smallest anode insulator. (middle) Size measurements of the smallest thermocouple available. (bottom) Provides the size constraint of the cathode wire [29].

As the number of detectors increases, the insulated wires fill the surrounding space in the flux wire tube which prevents the wire from bending. Also, four-hole insulators are less likely to bend due to the four anodes or thermocouple wires that will pass through. With the removal of the spring and reduction of the MPFD chamber, the new design of the array will allow for more MPFDs. The maximum number of MPFDs can now be determined with the available alumina insulator in Figure 2.3. In Figure 2.4, the left design shows a total of nine MPFDs and two thermocouples that can fit inside flux wire ports with diameters of 3 mm.

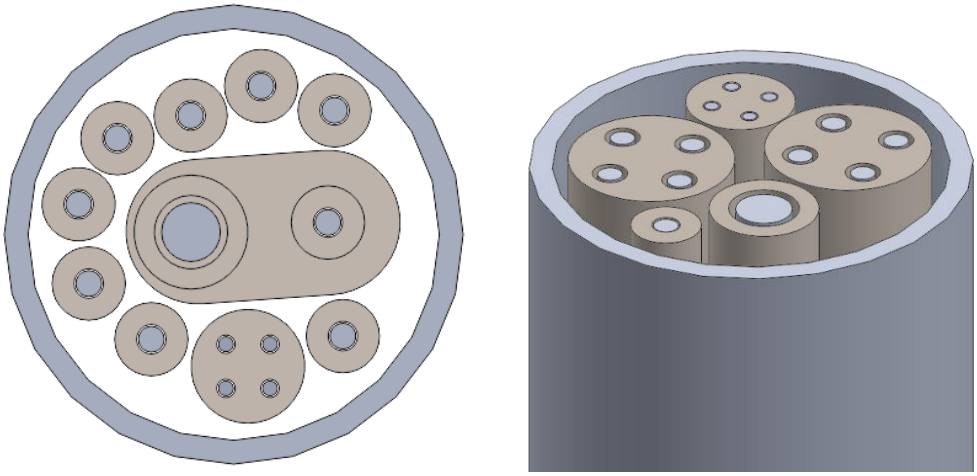

Figure 2.4: (left) The maximum number of MPFDs and thermocouples that can fit inside a 3 mm diameter tube. (right) The upper insulated wires that lead to the MPFDs inserted into the flux port.

The new design of the MPFD chamber and the changes made to the assembly will now allow for insertion into flux wire ports smaller than 3 mm. Figure 2.4 shows the upper assembly design of the MPFD array that uses multi-hole insulators to reduce the structural weakness of using single-hole insulators on all of the wires. Both single-hole and multi-hole insulated MPFD arrays are the current designs used for mock-up and in-core testing at KSU. The following chapter will focus on the method for fabricating MPFD arrays that can be inserted into a 3 mm wide flux port.

Chapter 3 - Micro-Pocket Fission Detector: Device Fabrication

MPFD arrays are fabricated using the materials discussed in the previous chapter and the final design shown in Figure 2.4. Information provided in this section will assist with development of a fabrication method that provides results and the best method for assembling a functioning MPFD array. Every array is tested and the results are used for modifying the fabrication process to improve the physical properties of the array and the detector performance. Discussed in this chapter are the preparation of the material, electrodeposition of the MPFDs, initial assembly methods, and the final assembly method.

3.1 Insulator Segmentation

Alumina insulator tubing is purchased in the longest lengths possible to lower the overall material cost. Alumina providers cut the pieces to length by using a diamond wire saw and charge an average of 2 cents per cut [29]. The lengths of the alumina ranged from 18 in to 30 in depending on the diameter of the insulator and the number of holes. In order to meet the design specifications for the detector arrays, the alumina is cut to lengths less than or equal to 0.5 in. Lengths for the insulator are chosen based on the material hardness and the bend radius of a dog-leg in the flux port tube. Diamond wire sawing or razor blade fracturing are the two methods of cutting used for preparing the insulator.

3.1.1 Fracturing and Polishing Method

Fracturing the alumina using a point shearing force delivered by a razor blade was the first method used for segmenting the insulator. Cutting methods utilized by alumina suppliers were not available at the time and fracturing provided prepared insulator the quickest. Detector arrays were needed for determining physical properties such as the maximum number of nodes,

the array flexibility, and its' durability. Therefore, other methods were not pursued until initial batches of alumina insulator were provided. Using razorblades, the alumina was cut to approximately 0.5 in lengths. Each type of insulator fractured differently and resulted in a variety of lengths. Single-hole insulator fracture lengths are between 0.5 in and 0.25 in. The wide range of lengths for single-hole insulators is a result of crushing. Crushing the insulator is avoided by applying just enough pressure to break it. Multi-hole insulators fracture between lengths of 0.5 in and 0.4 in. This type of insulator cannot be fractured below 0.4 inch with the current method. Cutting the insulator also creates jagged edges with a wide degree of severity and as shown in Figure 3.1 have little or no consistency.

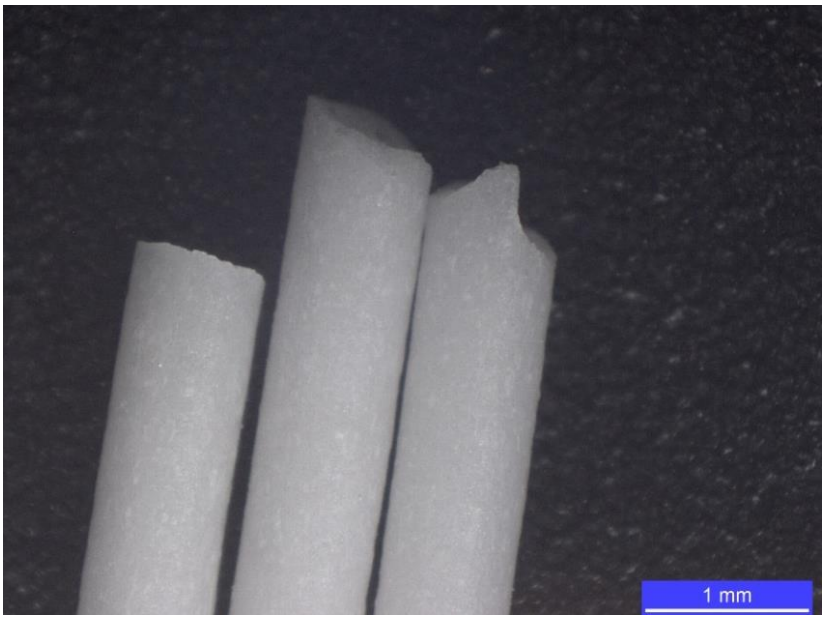

Figure 3.1: The variations in the jagged edge sizes caused by using the fracturing method.

Due to jagged edges, another step in segmenting the insulators is the polishing of the each insulator to reduce the severity. A diamond polishing pad grinds the jagged edges and helps with providing consistent lengths. Both fracturing and polishing the alumina insulator results in a loss of 1 in/ft of material. These results were adequate for the initial fabrication phase to provide a quick turnaround of material for the assembly process and understanding the limitations of the

detector arrays. After preparing initial batches of insulator, other methods for preparing the next batch of insulators were researched, specifically diamond wire cutting.

3.1.2 Diamond Wire Method

Alumina providers demonstrate that diamond wire cutting provides straight cuts with precise lengths [29]. After cutting the first batch of insulator, a process for cutting the insulator using a diamond wire saw was developed and is currently the preferred method. The diamond wire saw at S.M.A.R.T. Laboratory is used for preparing and cutting the samples. All of the same type of insulator is placed on a substrate and hot wax is poured onto the insulator. As the hot wax cools, it holds the insulator in place and allows for the insulator to be cut. Both ends of the insulator are cut to provide equal length cuts as shown in Figure 3.2. Use of the diamond wire saw allows for exact cuts less than 0.5 in and all pieces for this method have a length of 0.25 in (see Figure 3.2). A smaller length will improve flexibility for inserting the detector array and the straight cuts will fit together preventing voltage discharges or leakage current.

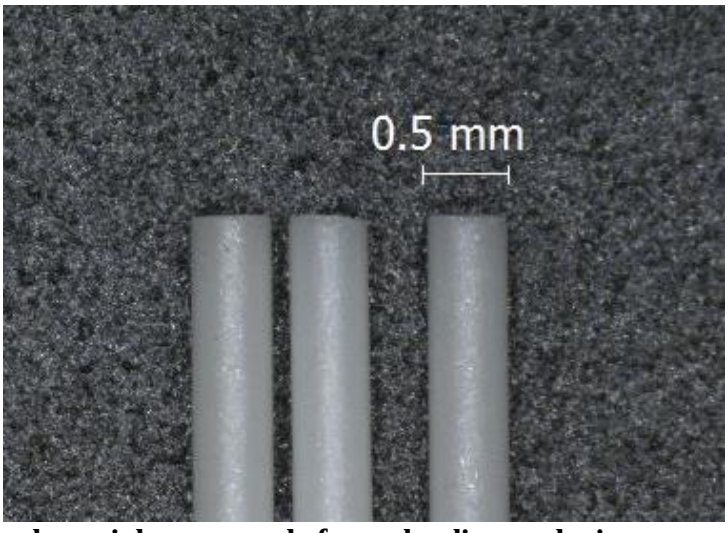

Figure 3.2: The equal, straight cuts made from the diamond wire saw.

Diamond wire cutting requires more preparation and cleaning than the fracturing method, thereby, increasing the production time. Despite the time increase, diamond wire saw provides

superior cuts and results. The extra time is spent removing the various contaminants added from the process. When cutting the insulator, the diamond wire saws require mineral oil that lubricates the blade. The contaminants introduced are removed by using alcohol for the mineral oil and boiling water is used to melt the wax. After the wax melts, the insulator can be fully separated from the rest of the contaminants. Before the insulator is ready for assembly, the alumina insulator is cleaned in a similar fashion to the fracturing method and is discussed in the following section.

3.2 Material Purification

An important part of the assembly process is to provide clean materials with little to no contaminants to prevent the production of unwanted isotopes. Anything placed within a nuclear reactor needs to have as few impurities as possible to prevent the chance of creating isotopes that could cause a significant radiation dose upon removal. Therefore, it is important that gloves are used to prevent contamination from any oils or other substances when handling any of the materials or detector arrays. Each material used for fabricating any detector array uses a specific cleaning method. Discussed in the following sections are methods on how the MPFDs, segmented insulators, and electrical wires are cleaned and prepared for assembly.

3.2.1 Segmented Insulators and MPFDs

Any contaminant introduced from initial material orders to an assembled detector array can be removed using an ultra-sonication process. Ultra-sonication uses sound energy to agitate the particles in a sample through a liquid medium. This process is used on the segmented insulators to remove dust from the diamond polishing pad, oils from the diamond wire saw, and other residues left from making alumina. After removing the mineral oil and wax from the segmented insulators, acetone is used as the cleaning medium for the sonication bath. Acetone is

a solvent that removes organic compounds such as grease, paint, and adhesives. Following the sonication with acetone, isopropanol is used as a cleaning bath to remove the residue left by acetone and the nonorganic contaminants in the samples. Finally, deionized water is used to sonicate the pieces for removing any left-over contaminant. These three baths are used on all insulators after it has been cut by the diamond wire saw or polished with the diamond pad. This process is applied to insulators that were used for a previous MPFD array.

Similarly, MPFDs are cleaned using ultra-sonication before and after the fissionable material electrodeposition discussed in section 3.3 is added. Unpolished MPFD pieces were sonicated to demonstrate that the normal cleaning method will not fracture the disk or spacers. No visible damage is present under a microscope even after a disk is attached to an array. Other tests were conducted using isopropanol to clean a freshly electrodeposited uranium and thorium sample. Isopropanol will sufficiently clean the MPFDs without removing the fissionable material or the platinum substrate. Acetone and deionized water is avoided in the sonication process to preserve the deposited material. Using acetone may result in the removal of fissile material, thereby, lowering the mass in the chamber. Also, deionized water takes a longer time to dry than isopropanol and if the water has not evaporated before testing, the chamber will continuously discharge voltage. Several of the issues prevented by proper cleaning are discussed in the assembly processes (see sections 3.4.2 and 3.5.2).

3.2.2 Electrical Wires

The last components left to clean before assembling the detector are the electrical wires used for the cathode, anodes, and thermocouples. Uninsulated wire is provided with a transparent sheath of plastic that protects the wire until it is soldered or removed by heat. None of the plastic can be allowed into a nuclear reactor and must be removed before the assembly

process. This plastic sheath also prevents good electrical contacts and prevents the measurement of current induced by a fission fragment. Therefore, a similar cleaning process to the alumina insulator is used for cleaning the wire. First, the wire is cut and clamped down on one end. Next, a cleanroom wipe is soaked in acetone and used to thoroughly clean the wire multiple times. This process is repeated with isopropanol and deionized water. During this process, the wire is straightened by firmly grasping the wire with the clean wipe and pulling it tight. Straightening the wire helps with assembling the MPFD array and is discussed in future sections (see section 3.4). Measuring the resistance of the wire before and after the cleaning showed that the plastic was removed during the cleaning process.

3.3 MPFD Electrodeposition

The final preparation before assembling the MPFDs is the electrodeposition process used to coat the disk substrates with fissionable material. MPFD electrodeposition is not the primary focus of this thesis and is only covered for completeness. Detailed information concerning this process is provided by "Electrodeposition of Uranium and Thorium onto Small Platinum Electrodes" (see reference 8). For the final MPFD design, one disk will use ^{235}U to detect thermal neutrons and the other disk will have ^{232}Th for breeding ^{233}U to extend detector lifetime. Electrodeposition is the process of coating a material with thin layer of metal and placing a different metal on top to modify the surface properties [30]. Coating the MPFD disk with a thin U and Th coatings consist of three steps: electrode fabrication, solution preparation, and electrodeposition [30]. Electrode fabrication for MPFD involves applying metal contacts to the alumina disk between the cathode and anode holes (see Figure 3.4). Metal contacts are added using an electron beam evaporator in the KSU S.M.A.R.T Laboratory. Positioning of the contact is controlled using custom shadow masks designed by KSU's Multiphase Microfluidics

Laboratory using a Minitech Mini-Mill 3 micro-milling machine [30]. Evaporated contacts consist of a 50 Å titanium layer and a 500 Å layer of platinum. The next step of the electrodeposition process is the solution preparation of the U and Th. Fisher Scientific 99.9% uranyl- and Strem Chemical 99.8% thorium-nitrate are used to provide the respective fissionable material [30]. Ammonium nitrate is added to the nitrates and placed on a magnetic stirring plate [30]. After several days, the solution precipitates material and the electrodeposition is conducted immediately after solution precipitation [30]. The final step is the electrodeposition of the precipitated solution onto the electrodes of the disks. Figure 3.3 illustrates the general setup of the electrodeposition station and process [30].

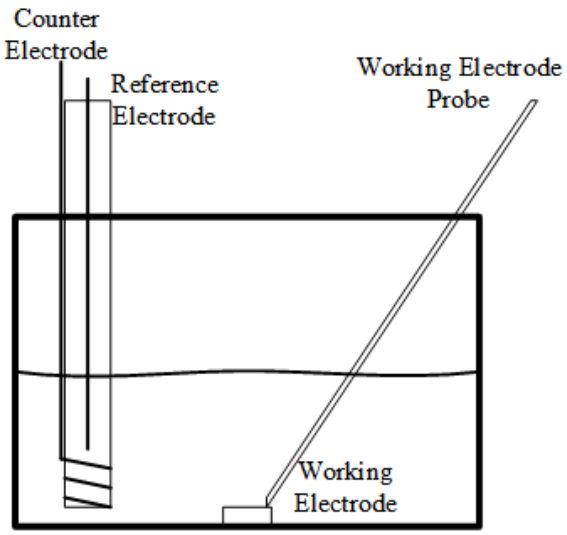

Figure 3.3: The apparatus of the electrodeposition process [30].

After cleaning the samples, a CH Instruments CHI600E potentiostat utilizes an electrochemical cell with three electrodes to deposit the U and Th [30]. The Electrochemical cell design accommodates the small electrodes and provides a 3-dimensional translation stage, counter/reference electrode assembly, working electrode probe, and a Leica DMS300 microscope [30]. As shown in Figure 3.3, the counter electrode is wrapped around the reference electrode glass vial and placed in a glass petri dish with the substrate [30]. Electrolytic solution

is added to the dish to cover the substrate and counter/reference electrodes. The working electrode probe is put into contact with the substrates electrode. After the working electrode comes in contact with the substrate, cyclic-voltammetry deposits the fissionable material on the working electrode surface [30]. Results of the electrodeposition process are shown below.

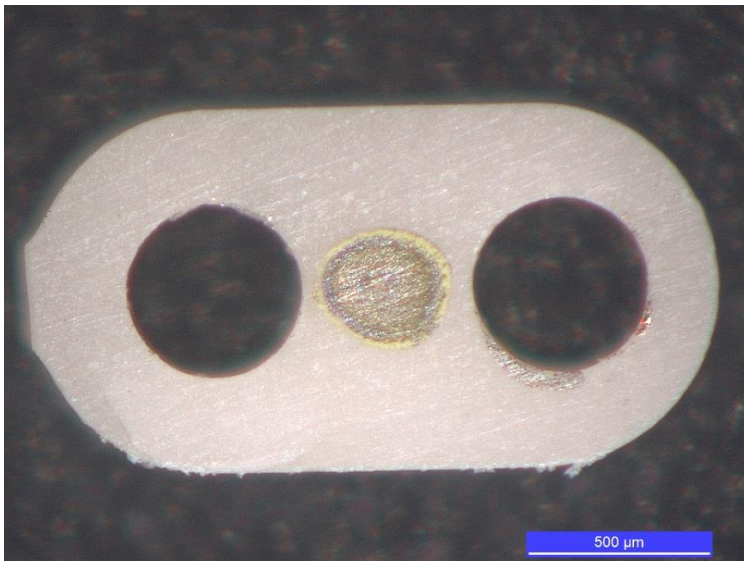

Figure 3.4: The final results of the uranium electrodeposited to MPFD disks [30].

As shown above, the electrodeposition deposits the uranium and thorium with precision. Uranium deposited on the disk electrode has a yellow tint and the thorium is transparent. This result is important for identifying which side of the MPFD has the U/Th material during assembly (see section 3.5.2). For more information on the overall electrodeposition process, the reader is deferred to the literature [30].

3.4 Initial Assembly Method

With all the materials prepared and cleaned, developing a method for assembling the detectors with consistent results and very little fabrication flaws was the main focus. The initial assembly method provided information about possible problems that can arise while building the MPFD arrays. This section describes the method of assembling the detectors and the results observed from the design.

3.4.1 Multi-Wire Assembly

The end use requires that every assembly have a length of 17 feet or longer to reach from the top of the KSU TRIGA nuclear reactor vessel to the core. For the initial assembly, an extra 10 feet of wire was added to compensate for the loss of wire during construction. Wire threaded into single-hole insulators is clamped to hold the wire in place. As shown in Figure 3.5, the wire is laid along the edge of laboratory tables and held in place by clamps. The tables are arranged to provide room for multiple wire assemblies and to accommodate the long wires. Single-hole insulator is added and pushed to one end of the wire. The smoothness of the wire determines how smoothly the insulator will slide onto the wire. If the wire contains plastic deformations, it will prevent the movement of the insulator and further damage the wire. Over time, the tip of the wire will weaken and bend depending on the smoothness of the wire. Cutting an inch off the wire provides straighter wire for further assembly. The extra wire is added to allow for the wire to be cut as many times as is needed. Upon completing a single strand of wire, the assembly was hung on a wall and protected with packing foam to prevent any damage while the remaining MPFD arrays were assembled.

Figure 3.5: The initial equipment setup for assembling MPFD arrays. Also shown are some apparatus needed to build the assembly.

Similarly, multi-wire insulator assemblies are constructed using clamps to hold the wire in place (see Figure 3.5). All the wires are strung up on the table at the same time and the wire ends are brought together. Each wire is strung through the multi-hole insulator one piece at a time to prevent wire crossing between the insulators. After inserting the first wire, the next wires are inserted in a clockwise manner to prevent any crossing of the wires. Inserting wires in a specific direction allows for more than one worker to assemble a multi-wire component without causing confusion or misaligned insulators. Regardless of what type of insulator is used, the tip of wire will weaken and bend which prevents the threading through the insulator. The wire is often cut to provide straighter wire and quicken the assembly process. Using the steps provided in this section, an array consisting of 2 four-hole anodes, a four-hole thermocouple, a two-hole thermocouple, a single-hole anode, and a cathode wire was produced. Each wire in the multi-hole nodes is separated by using single-hole anode insulator at the MPFD junction. Attachment and termination of the MPFDs is described later in the final assembly process (see section 3.5.2). The arrays described in this section were not used for testing and were used to provide information on the results of the assembly process.

3.4.2 Assembly Results

Several problems arise by assembling MPFD arrays with this initial method that needed to be avoided in future iterations. The most important problem is the wire damage and the plastic deformation resulting from both the addition of insulator and the clamps holding it. the wire that is fastened on the table shown in Figure 3.5 is bent at each clamp to an angle of 90°. Plastic deformation occurs at each clamp location which weakens the wire and eventually results in a wire breaking. If a wire breaks in a multi-node component, it must be removed and a new one threaded in its place. This will further weaken the other wires resulting in the possibility of

more wires breaking while assembling the array. Another problem of the plastic deformation is wire breakage as the insulator slides down the wire. Other wire damage includes the kinks caused by wire looping together before being pulled through the insulator (see figure 3.6). Pulling the kink through the insulator will break the wire and must be straightened before continuing. Finally, wire damage occurs from misalignment of the insulator hole (see Figure 3.6). Bringing the misaligned insulators together will cause the wires to twist and kink. The wire causing the issue can be removed and corrected, but the removal results in more damage to the wire. Due to multiple cases of wire damage, the final array is not straight and will prevent insertion into the flux test port. Also, any weak wires will most likely suffer mechanical failure during the insertion process. Despite the hardness of the alumina, the short pieces will follow the jagged direction of the wire.

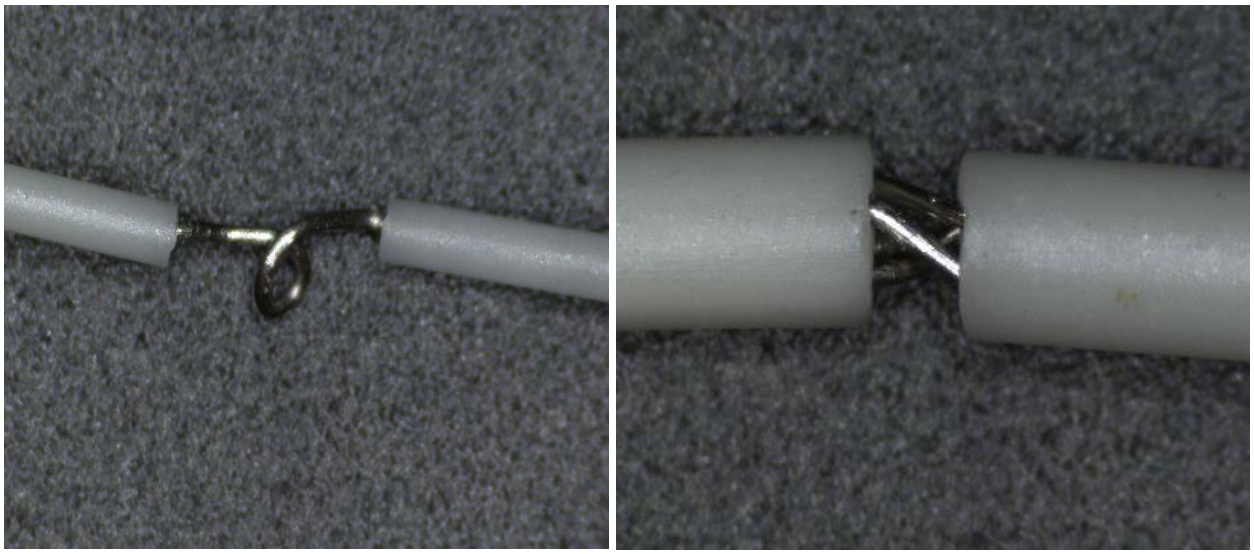

Figure 3.6: (left) Damage caused to the anode wire during the array construction. (right) The result of wires crossing between the insulators due to misalignment.

Another problem with this assembly method is the loss of material as a result of wire damage and use. Several feet are lost for every wire that is insulated and if not anticipated will produce an array that is too short and unusable. Finally, the four-hole thermocouple insulator has holes that do not meet the design specifications and the wire will not pass through easily.

The two-hole thermocouple insulator has the same design specifications, but the wire fits smoothly through the holes. Constructing a four-hole thermocouple array is currently not possible due to the weak chromel wires breaking. Therefore, four-hole thermocouple insulators will be removed from the assembly process due to the larger diameter insulator that is needed for the thermocouples. Overall this assembly process did not result in viable detectors that could be used for neutron detection or mock-up testing. Several weeks are required to build an array using this initial method and mistakes cause even more time loss. None of the MPFD arrays assembled from this method were tested in the mock-up or in the reactor for neutron testing. Also, any MPFD disk or spacers attached were removed to prevent their loss. Using the information provided in this section, a new assembly method was developed for superior MPFD arrays.

3.5 Final Assembly Method

All the arrays previously constructed were disassembled and cleaned using the methods described in a previous section of this chapter (see section 3.2). More materials were prepared for assembly and the lab space was rearranged based on the discoveries of the initial assembly method. The results also provide detailed information on how to avoid damaging the materials. Described in this section is the final assembly method used in the S.M.A.R.T Laboratory to create the current MPFD arrays for mock-up testing and in-core detector testing. All of the changes made below decrease the fabrication time of the arrays and allow for multiple arrays to be assembled at the same time. Included in this section is the array cleaning after assembly and the addition of PTFE shrink tube to change the physical properties of the array. All of these sections discuss the efforts of constructing reliable detector arrays for all types of testing. The

testing of the arrays will be covered in the next two chapters and will refer back to several of the changes made to the final array construction process.

3.5.1 Assembly Changes

Before changing the assembly process, the tables in Figure 3.5 were changed to provide 18 straight feet of desk space. Rearranging the tables reduces the work space; however, this new arrangement reduces the number of clamps needed to hold the wire (see Figure 3.7). Fewer clamps will prevent wire damage and allow for the wire to be clamped without bending it. Figure 3.7 demonstrates how the multi-hole insulators are now assembled. Each anode wire is threaded individually rather than all wires simultaneously. Individual threading can result in more wire crossing, but each insulator can be checked with the previous one to prevent misalignment. It also decreases the assembly time from several weeks to less than one week. As shown in Figure 3.7, the wire is fed by wire rollers as more insulators are threaded. In this process, a single anode wire holds the insulator in place and the other anode wires are moved. Another benefit is the wire will remain straight during the assembly process with only one bend at the very tip of the wire. Therefore, only two extra feet of wire is needed instead of 10 feet.

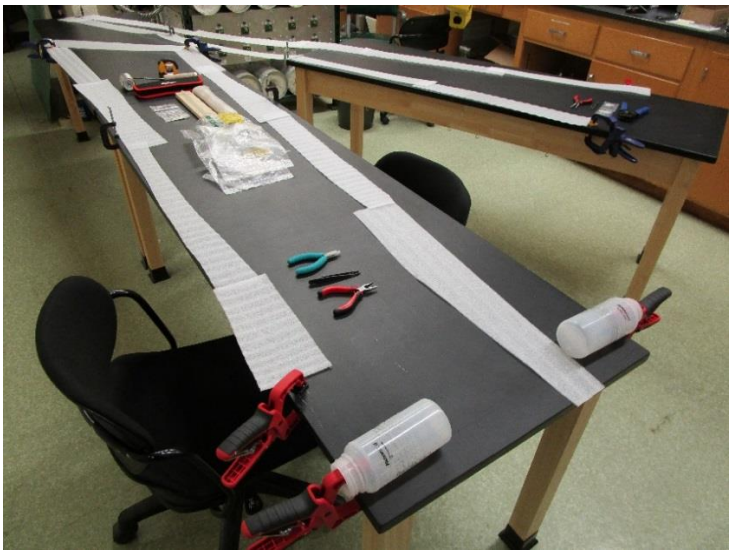

Figure 3.7: The rearranged assembly setup and how the wires are clamped down.

Changing the layout of the assembly and using straight wire did not help with the four-hole thermocouples. Analyses of the four-hole alumina insulator used for thermocouples show that the tolerances of the insulator holes prevents consistent wire insertion. If wire insertion fails during the assembly process, the alumina insulator is removed which increases wire fatigue. Also, the thermocouple wires are too weak to survive the wire cleaning process due to the tensile strength. Therefore, the thermocouple wires have the plastic protective sheath. Despite the plastic sheath, the wire is significantly small and weak resulting in the inability to thread the insulator. Smaller thermocouple wires were used to solve the problem, but the wire did not have the tensile strength to survive the threading process. Difficulty of adding the insulator resulted in the four-hole thermocouples being removed from the design. Further development of the thermocouples is discussed in the results of the mock-up testing (see section 4).

Several other changes are currently used to construct MPFD arrays due to the straighter wires provided by the previous changes. Metal tweezers are used to grip and push the wire through the insulator. This is currently done for the 3^{rd} and 4^{th} wire of the four-hole insulators and the second hole of two-hole insulators. The holes of the insulator are aligned enough to allow wire to slide through several insulators at one time. Adding several insulators at once cut the assembly time in half for multi-node arrays. Assembling a nine node MPFD array with a single thermocouple takes approximately 24 hours of construction time with the new assembly method. The MPFD arrays produced using this method are straighter and contain little to no wire damage (see Figure 3.8). All MPFD arrays used in mock-up and in-core testing were assembled using this method. As shown in Figure 3.8, the array will tend to stay straight and flexible enough for insertion. Finally, the wires at the end of the array are straight enough to insert detectors without the wire breaking and losing MPFDs.

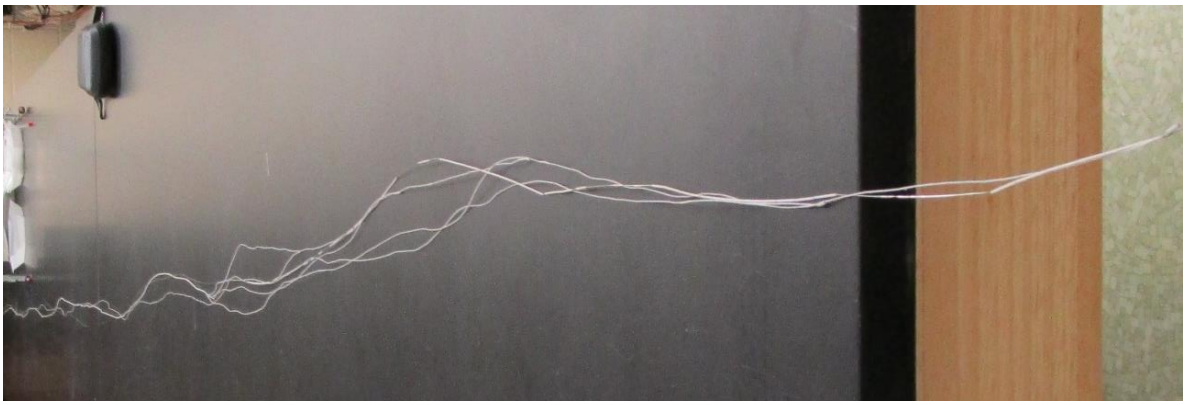

Figure 3.8: The final array using the new assembly setup.

3.5.2 Attaching MPFDs

After constructing a reliable array, the next step is attaching the MPFDs. There are two types of MPFDs used for testing. The first type consists of two polished disks and one polished spacer as shown in Figure 2.2. These MPFDs are polished to provide better electrodeposition results and are used for the in-core neutron testing. A second type of MPFD uses only rough disks and spacers for mock-up testing. Rough MPFDs are used for mock-up testing because of the cheaper cost than the polished MPFDs. However, the assemblies for both types of MPFDs use the same process and the smoothness does not affect it. Terminating the MPFDs without using any adhesive material or binding agents lowers the inventory of radioactive isotopes and increases the long term reliability of the connection. The MPFDs are attached to the extra length of wires left after the assembly of the insulator (see Figure 3.8). Spacing of the MPFDs is controlled by adding or removing anode insulators on the array and cathode insulator hold the MPFD chamber together. Experimenting with the disks and spacers showed that the individual pieces are weak and prone to fracturing from shearing forces. The small disk and spacers build up static charge increasing the possibility of losing detectors. Electrostatic discharge bags and carbon fiber tip tweezers are used to prevent charge build-up and handle the components. MPFDs are strongest when placed together on the wire and will not break unless the cathode and

anode wire are pulled in opposite directions. Placing the disk and spacers on the wire is very difficult and can result in lost pieces and even damaging pieces. Once the MPFD is assembled on the array it can be held in place by any of the insulators. The preference is to use single-hole anode and cathode insulators to hold the MPFDs in place. Using four-hole insulators will possibly result in the breaking of MPFDs due to the way that the insulators have to be bent around the MPFD. When placing the detectors on the wire, the spacer is aligned correctly with the disk so that the deposited uranium and thorium is not covered by the spacer. Any change in the alignment and space of the chamber will result in a reduction in neutron events and the energy deposited.

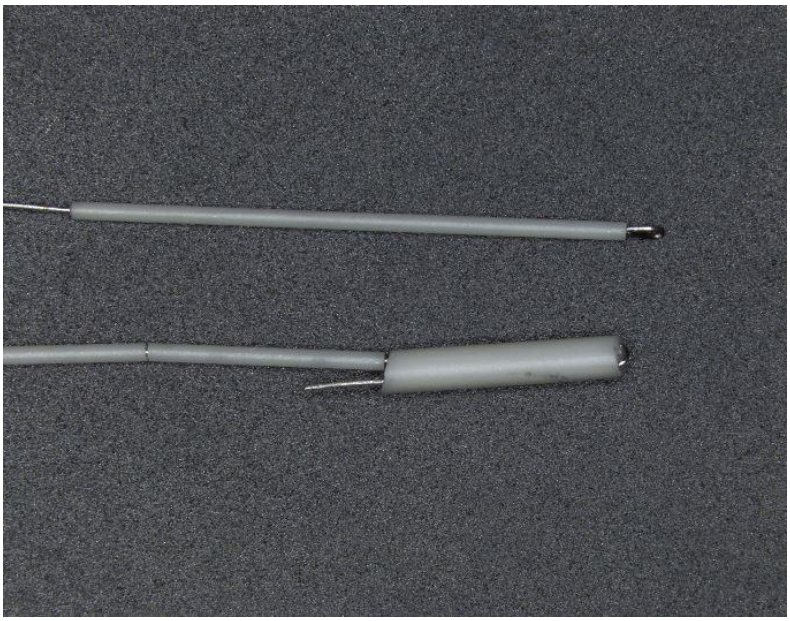

Figure 3.9: (top) The current cathode termination method. (bottom) The four-hole anode termination method.

After attaching the MPFDs, one of two methods is used to terminate the MPFD wires. The first method uses a single-hole insulator and the leftover wires are bent over so that the insulator cannot slide pass the created joint (see Figure 3.9). A second method uses a four-hole anode and loops the wire down the insulator and back up through one of the other holes. This method does not crimp the wire or structurally weaken the wire. Tests on the two methods

showed that single-hole terminations result in the wire breaking at the crimped joint. Four-hole anode termination sites show that the wire will break somewhere along the wire itself and never at the joint. Therefore, the second method has strength equal to the tensile strength of the wire. Anode termination sites always use the second method, but the cathode must utilize the first method. Results of attaching the MPFDs are shown in Figure 3.10. The size of the cathode wire allows for the insulator to be stopped by the crimped wire and not the joint. This means that the wire will also break elsewhere instead of the joint. This result is good because acquiring multi-hole insulators the size of the cathode is not viable for the mock-up insertion test.

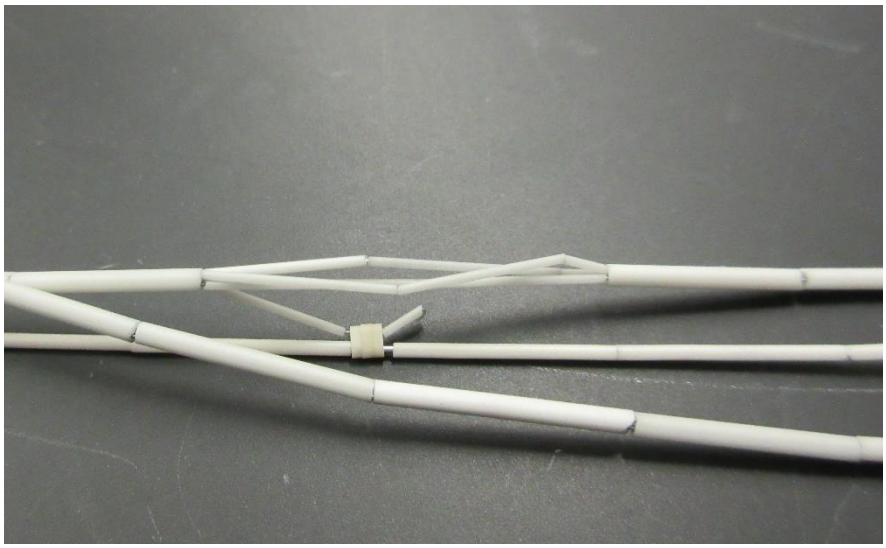

Figure 3.10: Demonstrates the final MPFD assembly with combined nodes for combining the array and adding structural integrity.

Another step included in larger assemblies is the use of the vacant holes in the multi-node termination method (see Figure 3.10). By combining several individual strands of the anodes, the structural integrity of the array is increased and it prevents separation of the wires. To assemble the array in this method, a four-hole insulator termination has a different wire pass through an empty slot of the insulator. Before reaching its respective MPFD, single-hole insulator is added until it reaches the detector. It is important to remove all slack in the MPFD array to prevent insulator from bunching up from the insertion process (see section 4). This

method is only utilized for large quantities of nodes to prevent the insulator wires from twisting and preventing insertion of the array. The final step of assembly is to add the connectors to the top of the array (see section 3.6)

3.5.3 Ultrasonic Cleaning

An assembled MPFD array does not function as neutron detector until it is fully cleanedin an ultrasonic bath. During the assembly method, the components of the detector array are contaminated with nickel wire shavings and other foreign objects. Nickel shavings are a result of the soft metal wire (nickel) passing through hard insulator (alumina). On the Mohs scale, alumina has a hardness of 9 and nickel has a hardness of 4 [31]. The amount of nickel shaving is reduced by the final assembly, but even a small amount of nickel shavings cause noise issues when detecting neutrons (see section 5.3). Shavings from the wire are statically charged to the insulator and collect mostly on the outer edge (see Figure 3.11).

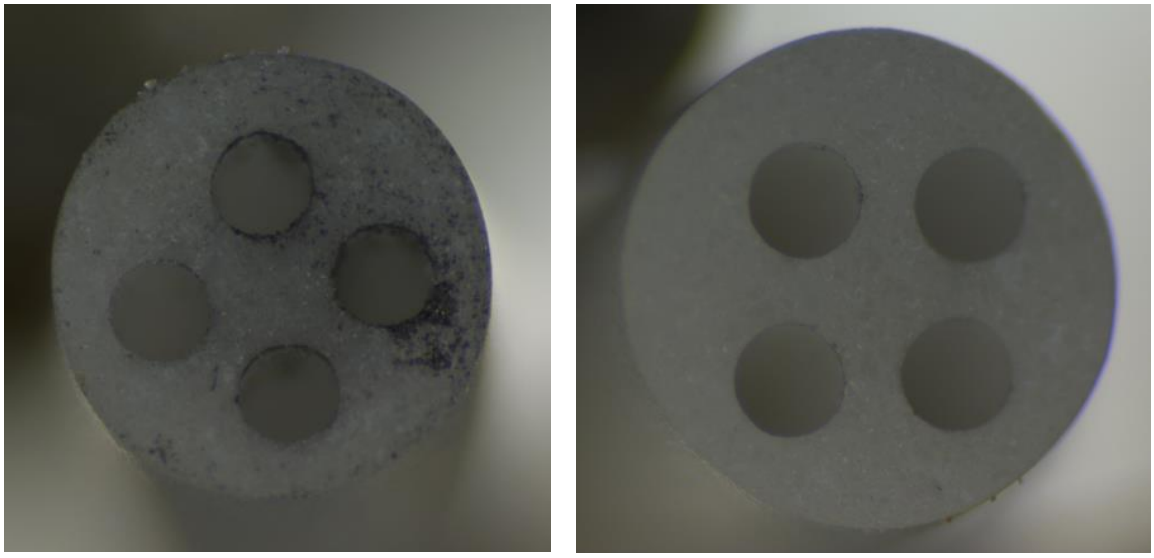

Figure 3.11: (left) The alumina insulator contaminated with nickel shavings. (right) The same alumina insulator after ultra-sonicated with isopropanol for 15 minutes.

This effect is shown in Figure 3.11 and the subsequent result of cleaning the insulator. Ultra-sonication removes nickel shavings very well and only requires an isopropanol solvent.

Cleaning the individual insulators will remove the nickel shavings, but the insulator is attached to the array at this point. Therefore, the entire array is sonicated using this method. However, the insulator must be separated on the wire enough to allow for removal of debris between the pieces. If the insulators are not separated, nickel shavings will still remain. After the array is cleaned, the spacing needs to be removed to prevent bare wire from being exposed. This procedure will result in further sliding the insulator and causing more nickel shavings. The best method is to clean several feet for 15 minutes and slide the insulators towards the MPFDs. Depending on how straight the wire is, two to five feet of insulated wire can be cleaned at once and the space between the insulators removed without causing nickel shavings.

3.5.4 PTFE Shrink Tube

Following the cleaning process, the PTFE shrink tube may be added. The need for PTFE surrounding the array depends on what properties the MPFD array needs and the intended purpose. Purposes of the PTFE include isolating wires for troubleshooting, reducing the coefficient of friction, or protecting the array from damage. Adding the shrink tube must be performed carefully. Any movement in the insulator will create nickel shavings and may degrade detector performance by introducing noise. PTFE will slide on easily, but it can occasionally catch the edge of an insulator. Caught insulator will cause other insulators to move as well. A heat gun is used to shrink the tubes onto the array. Holding and clamping the array down will straighten the detector and allow the PTFE to hold it in that position. Any PTFE heated onto the detector array pulls the individual strands together and holds the array in the intended position. If the shrink tube must be removed, it can be cut away and the array can be cleaned again for reassembly. Regardless whether or not PTFE is added, the MPFD arrays used

for mock-up testing were ready for testing and did not require electrical connectors. All in-core arrays complete the fabrication process with the addition of electrical connectors.

3.6 Electrical Connectors

Upon completing the in-core arrays, connectors need to be added to deliver the signal to the measuring equipment. The connectors are always added at the end to allow for removal of any slack in the detector lines. Removal of the slack will prevent kinks during insertion or breaks in the nickel wire. Several times BNC or SHV connectors are attached to the array for convenience and easy connection to measuring systems. These are not the type of connectors that will be used in the final assembly and are not included in the final design of the array. For testing, the BNC and SHV connectors remove several variables and allow for noise analysis (see section 5.3). In this section, the final electrical feed-through system and connectors are provided. It will allow for the tube to be purged and filled with argon to any needed pressure. Also, the method for attaching connectors will be discussed due to the complication of connecting to the nickel wire or thermocouples.

3.6.1 Electrical Feed-through

Regardless of the flux tube that the MPFD array is inserted into, all tubes will be enclosed with a pressurized argon atmosphere. Swagelok is used to attach to the tube and MDC parts are used to provide the electrical feed-through [32, 33]. Adaptors to 0.25 in are available for flux tube diameters less than 0.5 in. After the tube is converted to 0.25 in Swagelok, Swagelok tees and valves are added to allow for an argon purge system (see Figure 3.12). One or two of the valves can be used for a vacuum pump to purge the flux tube and an argon to back fill the flux wire tube.

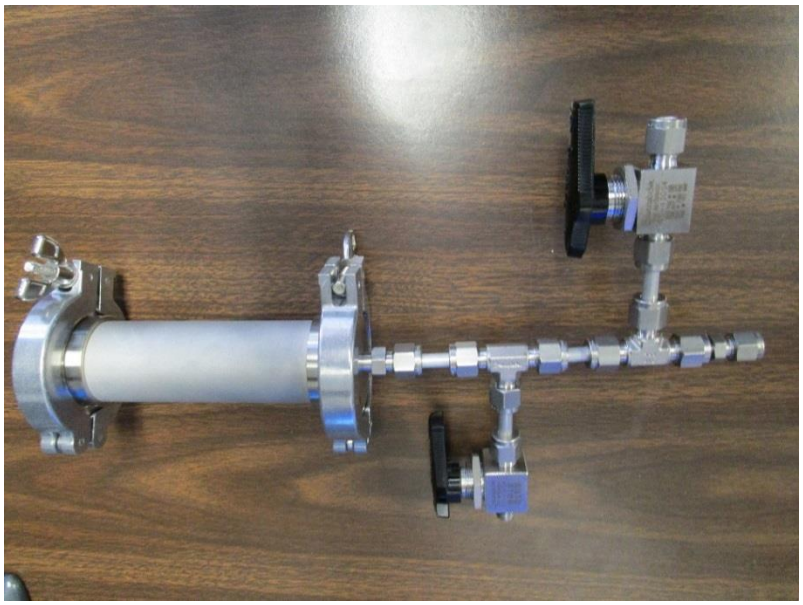

Figure 3.12: Details the electrical feed-through design with the argon purge system.

Finally, an adaptor from Swagelok to Kwik flange is used to attach the electrical feed-through. The feed-through uses connector pins which allow for the array to connect to the other side of the feed-through. Both components are shown below in Figure 3.13. All vacuum parts use Kwik flange connections for easy removal.

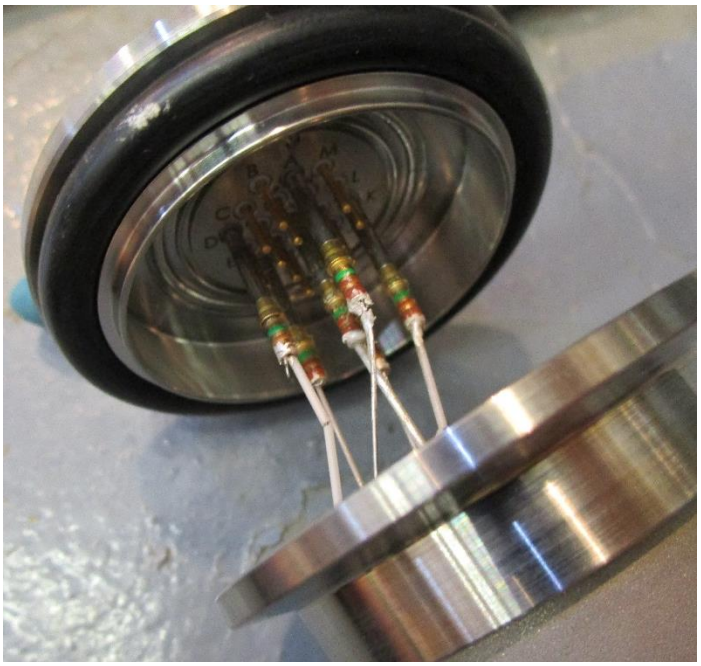

Figure 3.13: The electrical feed-through for in-core testing and the electrical pins used to connect to the measuring equipment.

3.6.2 Connector Attachments

The final step of assembling the in-core detectors is adding the connectors shown in Figure 3.14. Despite the type of connector used, the wire used in the array was not easily soldered to the connection. An oxidation layer prevents solder from bonding with the nickel. A two part silver epoxy was originally used to join the connectors to the electrical wires [34]. Silver epoxy requires several hours of preparation and needs to cure at higher temperatures to allow for the desired electrical properties. During this process, the array has to be moved to the furnace and the result of moving the detector could damage it. The epoxy method takes time to apply and the contacts do not provide the structural integrity desired from the electrical connectors. Therefore, much effort was spent determining the best method for connecting the array to the electrical feed-through pins. The method decided upon was connecting with an acid flux core solder [35]. Acid flux strips the nickel oxide long enough to attach the solder to the wire. Acid flux solder connections are very strong and will take more damage than silver epoxy before breaking. Figure 3.13 shows the result of using acid flux solder on the nickel wire and the connectors.

Figure 3.14: The use of acid flux solder to connect nickel wire to the pin connectors for the electrical feed-through (bottom) and BNC connectors (top).

Chapter 4 - Micro-Pocket Fission Detector: Flux Port Mock-Up

Determining the maximum number of MPFD nodes and physical capabilities of the array requires using a mock-up of the flux port tube. Mock-ups are a safe, reliable method for testing the physical properties of the arrays. Using the in-core test port may cause neutron activation of the array or fracturing that leaves pieces in the tube. The mock-up provides information on: the maximum number of MPFDs, intensity of the friction, possible damage sites, and complications with array insertion. Discussed in this chapter are the mock-up construction and the results from testing the MPFD arrays.

4.1 Mock-Up Construction

A full mock-up has a total length over 18 feet to ensure that the detector can reach the reactor core. It was constructed in reactor bay of KSU's TRIGA Mark II and mounted to the railing located at the thermal column of the reactor. This location provided room for inserting the MPFD array and for locating problem points. Covered in the following sections are the design of the mock-up, the material used, and the assembly of the test port.

4.1.1 Flux Port Design

A flux port tube inserted at a nuclear reactor contains several bends to prevent radiation streaming. Radiation streaming is the result of replacing the original shield/moderator with a weaker shield that allows radiation to travel unimpeded through the material. The sharp bends used in metal tubing are referred to as doglegs. The radiation must pass through some of the biological shielding instead of streaming through the tube. Unfortunately, doglegs also prevent the use of long pieces of alumina insulator and predetermine the length of the alumina pieces. Figure 4.1 shows the general design of the mock-up test port that is currently used. In Figure

4.1, the tube uses a large radius bend followed by several small doglegs. These bends are added to provide realism to how a test port is placed in a nuclear reactor. A flux test port may contain several bends to avoid hindering control rod movement or other equipment used in the reactor.

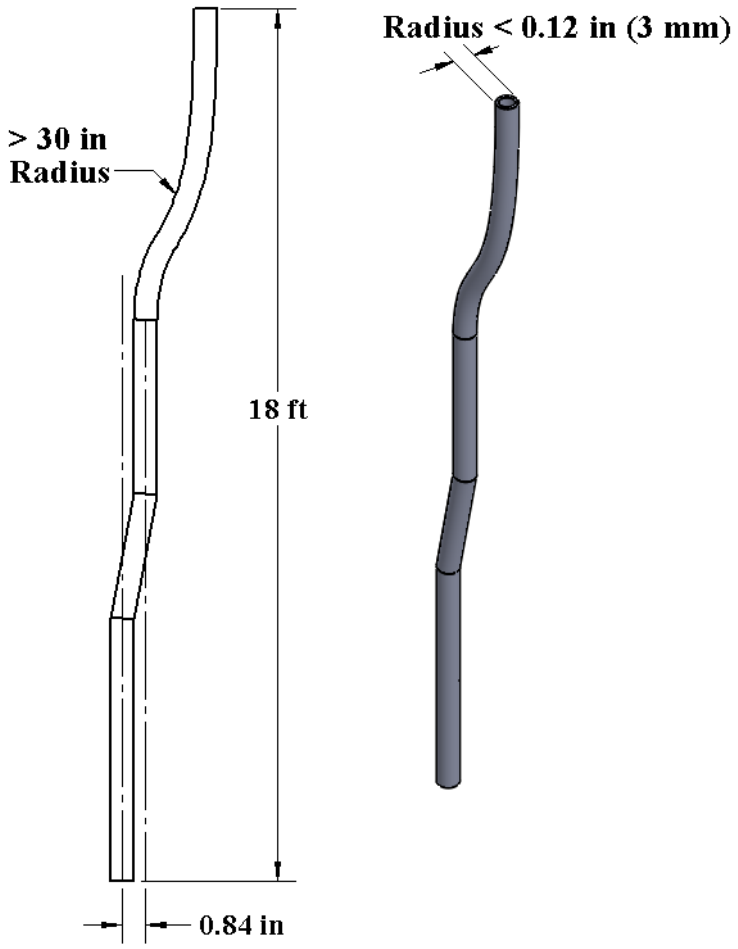

Figure 4.1: The mock-up test port design and the general dogleg used for preventing radiation streaming.

As shown in Figure 4.1, the mock-up has an initial curved bend with a radius greater than 30 in and several small straight bends with angles ranging from 5° to 7°. The mock-up has multiple tubes mounted in the same layout. Different types of materials are used for flux port tubes at a nuclear reactor and the goal of the mock-up is to understand how changes in the metal affect the insertion process. Aluminum, Inconel 600, and plastic are the three tubes used in the mock-up. Both aluminum and Inconel are commonly used at nuclear reactors due to the

radiation hardness of the materials. A transparent plastic tube is included in the mock-up to allow viewing of the array as the detectors are inserted.

4.1.2 Flux Port Material and Assembly

Other materials needed for the assembly of the mock-up include a 24 foot piece of 6" x 1' wood. All three types of tubing have a 3 mm ID as specified in the design constraints (see chapter 2). Only the plastic tubing was unavailable in the required 18 foot length. Adhesive shrink tube, bracketing clamps, metal tubing, and mounting screws were used to mount and connect the tubing. All of the materials were used to assemble the mock-up shown in Figure 4.2.

Figure 4.2: The completed mock-up mounted to the thermal column at the KSU TRIGA MARK II nuclear reactor.

Stencils of the tube design were placed on the wooden board to show where the tubes were mounted. All three tubes start at the top of the wood and terminate 18 feet below. Plastic tubing was mounted first using the bracketing clamps and mounting screws. Next, all 18 feet of the aluminum tubing was connected together using large tubing with an ID greater than the OD of the aluminum. Adhesive shrink tubing was added on top of the connecters to hold the parts together (see Figure 4.2). The aluminum tube was bent by hand and mounted to the wood just as

the plastic tubing. Finally, the Inconel tube was attached using similar methods. The final assembly of the aluminum and plastic tube are shown in Figure 4.2. After attaching the tubes, the entire mock-up was attached to the thermal column with U-bolts and the bottom of the mock-up was held steady by lead bricks.

4.2 Mock-Up Testing

The initial MPFD arrays were tested using the flux port mock-up described in the previous section. Results from these tests provide insight into designing better detectors that can utilize the smallest tube possible without reducing the structural integrity. A successful mock-up test occurs when an array inserted into the tube and exits through the tube, followed by removal without damage. Discussed in the following sections are the best method for inserting the arrays, results of the insertion, damage from the insertion, and improvements made to the array.

4.2.1 Inserting Arrays

Several insertion attempts were made before identifying the preferred insertion method. Each rough MPFD array is taken to the 22 foot level of the KSU TRIGA MKII facility and straightened out on the floor with the detectors near the mock-up. Two people are needed to handle the array. One person will hold and feed the array so that the second person can insert and push the array down the tube. For the initial insertion, each MPFD is carefully placed in the tube. After the active detector region is inserted, pressure is only applied to the cathode wire and multi-hole insulators. Both insulators provide the structural integrity of the MPFD array. Applying pressure to the single-hole anode insulators causes the wire to kink and the insulator to bunch up. Any kinks or bends will prevent the insertion of the array into the flux port tube. An example of the insertion process is shown below (see Figure 4.3).

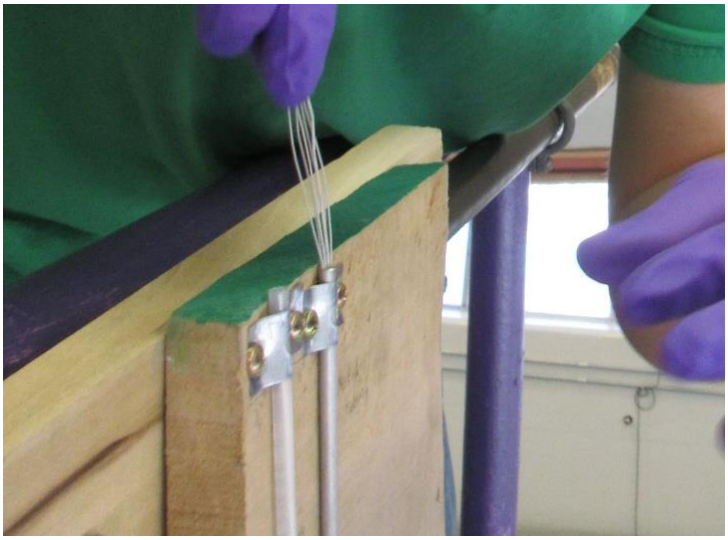

Figure 4.3: Shown is the method for inserting the MPFD array into the flux wire port.

Single-hole MPFDs are loosely held while pressure is placed on the cathode and four-hole insulators if available (see Figure 4.3). The individually-insulated wires are pulled down the tube by the connected MPFDs. Depending on the design, the array will stop and pushing will result in damage. This problem is avoided by pulling the array up a couple of inches and pushing again to gain momentum.

4.2.2 MPFD Limitations

In chapter 2, the design constraints show that a maximum of 9 MPFDs with a common cathode and 2 thermocouples can be inserted into a 3 mm diameter hole. The first MPFD arrays tested in the mock-up had the maximum allowable number of detectors and one thermocouple. None of these arrays were successfully inserted. As previously discussed, the insulator and wire twisted, thereby, preventing the insertion of the array. Also, the friction between the insulator and the side wall stopped the insertion process. Only three feet of the arrays made it into the test port for these designs. Therefore the thermocouple was removed from the design and the number of MPFDs was reduced. Successful insertions did not occur until three MPFDs were left. Single-hole insulator was used for each anode wire and the cathode wire was bare except at

the MPFD locations. Despite the difficulty of inserting the arrays, every failed and successful array was easily removed without damage, showing that the tensile strength of the anode and cathode wires is sufficient to permit safe removal of the MPFD arrays even in the presence of a significant amount of friction. Arrays placed into the plastic tube show that the damage occurs during the insertion. Several tests conducted on a four-node detector showed that a string of four-hole insulated wires could not be inserted due to the friction and size of the insulators. Tests also showed that using single-hole insulator failed because the force required to send the array down the tube caused plastic deformation to the cathode. Therefore, the maximum number of MPFDs for a 3 mm diameter tube is presently limited to three.

4.2.3 Damage Results

Insertion of the array results in two main possible types of damage. The first type is caused by applying force to the array and causing a local kink. This kink/bend is removed before continuing, but the damage to the wire is permanent. Figure 4.4 shows the damage from pushing the four-hole insulator down the tube and exceeding the strength of the insulated wire.

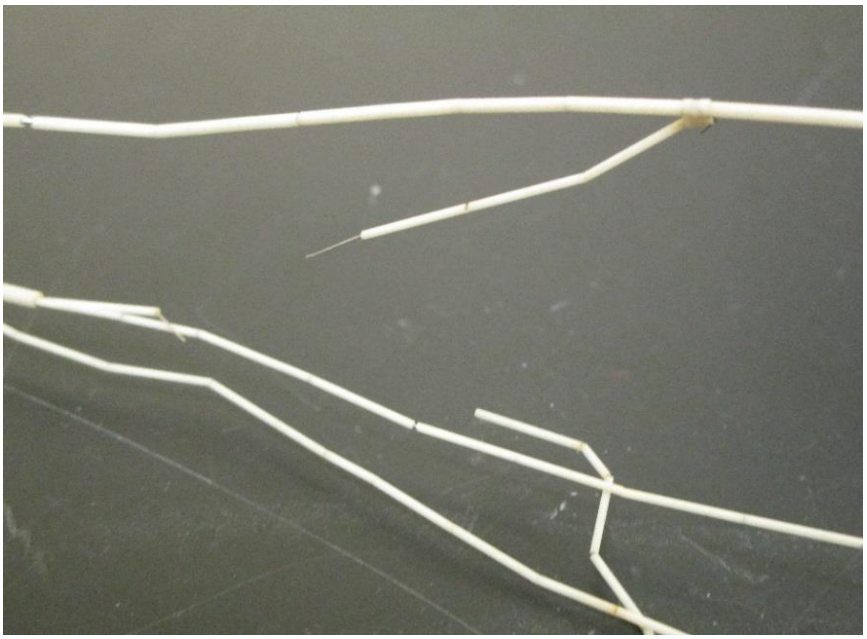

Figure 4.4: Details of the broken wires and bent insulator from a failed mock-up test.

If the array is reinserted, the damage sites will further degrade under smaller forces than originally applied. Therefore, the ability of reinserting MPFD arrays is dependent on the damage caused by each insertion. The other damage is the result of transiting from a four-hole insulator to single-hole insulators. Each detector is spaced vertically and insulator is placed on the wire up to the node. Commonly, assembly methods use four-hole insulators wherever possible to reduce the assembly cost. The rest of the wire is covered with single-hole insulators. If the wire is not cut to the exact length, insertion into the flux port tube causes the array to straighten and all of the slack is collected at the four-hole and single-hole junction (see Figure 4.5). Significant slack will prevent the array from being inserted as shown in Figure 4.5, but less slack will fit into the tube and cause an increase in friction from sliding on the tube wall. These wires either break after two or more insertion attempts or severely bend when pressure is applied.

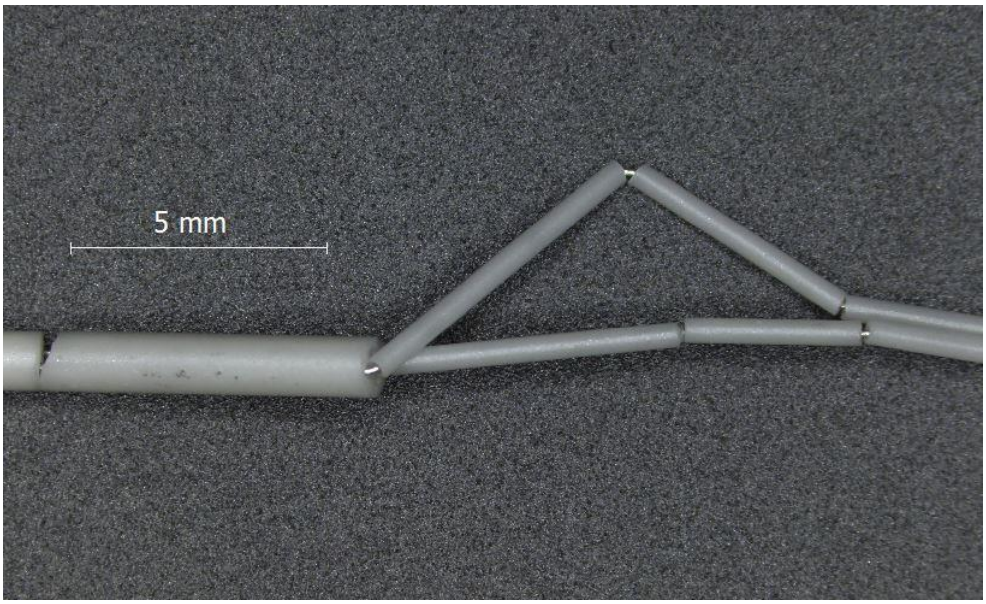

Figure 4.5: The result of inserting an MPFD array that has slack in an anode wire into the mock-up.

4.2.4 PTFE Arrays

Results from mock-up testing show that the difficulty of inserting an array depends in large part on the coefficient of friction. Each MPFD array inserted into the three types of flux

ports provided different resistances upon insertion. Aluminum tubes and alumina have a high coefficient of friction compared to plastic and Inconel tubing. Therefore, the same array can be inserted further down the Inconel tube than the aluminum tube. In order to increase the number of MPFDs, the coefficient of friction must be lowered. To lower the friction, PTFE shrink tubing was added to an array (see section 3.5.4). The use of PTFE allowed the number of detectors to be increased to 5 and also allows for the four-hole anode insulator to be used. Also, the PTFE adds structural integrity which prevents damage during insertion (see Figure 4.6). Despite the increase in detectors, PTFE will not survive the high radiation field present in a nuclear reactor. This means the actual working array cannot be insulated with PTFE in the active region of the core. There is still work to be done to determining the maximum number of nodes possible using only partial PTFE on the array.

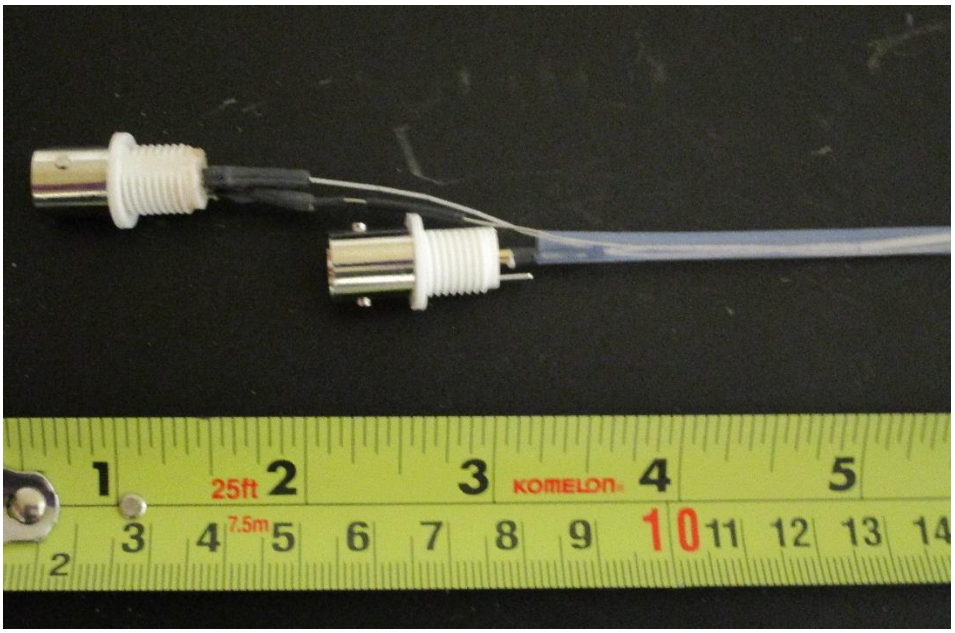

Figure 4.6: The PTFE shrink tube is attached to the array to provide structural integrity and lower coefficient of friction.

Chapter 5 - Micro-Pocket Fission Detector: Device Testing

MPFD arrays constructed for in-core testing use the polished uranium and thorium disks from the electrodeposition process. Each MPFD has a neutron flux response determined by the amount of uranium used, the location of the detector, and the amount of electronic noise. Evaluation of the detectors in this section is based on the following test plan. The flux at each test location in the KSU TRIGA Mark II nuclear reactor is measured from an iron wire flux calibration. Following the flux measurement, the MPFDs are tested for noise interference and non-neutron events. A final analysis of the detectors will cover the neutron sensitivity and determine if the new MPFD design is capable of long-term operations within a PWR.

5.1 Iron Wire Flux Calibration

Two locations were available for testing in the TRIGA Mark II nuclear reactor at KSU. The Intra-Reflector Irradiation System (IRIS) was first used for detector testing and it is located in an annular well in the radial graphite reflector. IRIS is a new facility that allows sample insertion into six air-filled aluminum tubes and is estimated to provide a constant 10^{12} n/cm^2·s total neutron flux. A water-filled tube that starts at the top of the reactor containment vessel terminates an inch below the center of the reactor core is the second location. This tube is referred to as the central thimble and it provides an estimated thermal constant flux of 10^{13} n/cm^2·s and a fast flux of 1.2×10^{13} n/cm^2·s at 250 kW. If the reactor is operated in pulse mode, the central thimble neutron flux can reach 10^{17} n/cm^2·s for several milliseconds. Utilizing the central thimble requires a 220 in long stainless steel 0.25 in diameter tube attached to an electrical feed-through, and the argon purge system (see section 3.6.1). These two locations provide various ranges in flux and allow for easy insertion into the reactor core. Prior to the testing of the MPFDs, the thermal and fast neutron flux for both locations will need to be

determined using the iron wire flux calibration method. This method will provide the flux per watt of thermal power over a region of where the detectors are located axially in the reactor. All equations and derivations used for calculating the flux calibrations are provided in Appendix B along with a set of procedures for determining the calculations. Calculations for both the IRIS and central thimble are determined in the sections below using the information provided in Appendix B.

5.1.1 IRIS Flux Calibration

Samples are inserted into the IRIS by using a plastic containment tube that is attached to a retractable wire. The plastic tube is four inches long and is encapsulated to prevent the leaking of radioactive materials. To determine the flux in the IRIS, the plastic containment tubes were used for inserting the bare iron wire and the cadmium covered iron wire (see Appendix B). Two four inch long pieces of iron wire were cut to fit the capsule. One of the wires was left bare and placed in the IRIS port #6 and the other wire was covered in cadmium to measure the fast flux of the reactor and placed in the 5^{th} port of the IRIS. Different flux ports were used to allow for both wires to be irradiated at the same time. Modeling showed that the difference in the flux at the two locations is minimal due to the close proximity of the wires and the radial uniformity of the reactor core. Both wires were irradiated for two hours at a thermal power of 200 kW. Using the procedures outlined in Appendix B, the thermal and fast flux of the IRIS ports were calculated and are listed in Table 5.1. A 20:1 ratio of thermal to fast neutrons is present in the axial center of the IRIS. The total flux of the IRIS at any of the four locations was expected to have an order of 10^{12} n/cm^2·s, but the results of the iron wire calibration show a smaller flux by an order of magnitude. This difference between the actual flux and the theoretical flux is possibly due to the installment of the IRIS or other changes made to the reactor core configuration. Differences

between the actual and theoretical fluxes will not affect detector testing and is only provided to show how the flux per watt calculations can change over time.

Table 5.1 The calculated IRIS flux from the flux wire experiment.

IRIS Flux Calibration						
Bare Iron Wire						
Wire Segment	Length (cm)	Mass (g)	Activity (μCi)	Act. Uncertainty (μCi)	Thermal Flux ($n/cm^2 \cdot s$)	Uncertainty ($n/cm^2 \cdot s$)
1	2.1	0.1908	6.113E-02	1.20E-03	2.199E+11	4.42E+09
2	1.7	0.1472	5.159E-02	1.02E-03	2.419E+11	4.95E+09
3	2.4	0.2145	7.620E-02	1.48E-03	2.466E+11	4.95E+09
4	2.0	0.1781	6.384E-02	1.27E-03	2.366E+11	4.90E+09
Cadmium Covered Iron Wire						
Wire Segment	Length (cm)	Mass (g)	Activity (μCi)	Act. Uncertainty (μCi)	Thermal Flux (n/cm^2·s)	Uncertainty (n/cm^2·s)
5	2.2	0.1935	3.722E-03	8.87E-05	1.510E+10	3.68E+08
6	2.2	0.1887	2.954E-03	8.26E-05	1.229E+10	3.49E+08
7	2.4	0.2029	2.973E-03	8.42E-05	1.150E+10	3.31E+08
8	1.8	0.1658	4.755E-03	1.40E-04	2.252E+10	6.74E+08

In Table 5.1 Wire segment 1 and 5 are referenced as the top of the pieces of bare and cadmium covered iron wire. Flux calculations in Table 5.1 shows that center of the core is located at the largest thermal flux in the third wire segment. This is the preferred location for testing the MPFDs and has a thermal flux of 1.233×10^6 $n/cm^2 \cdot s \cdot W$. Fast flux calculations show irregular distribution of the fast flux and the reasons for these results are currently unknown. Finally, the uncertainty of the calculated flux in Table 5.1 will have an average 2% of error. The error of the measurement is limited by the efficiency calibration used for the germanium detector and it could be improved upon by increasing the measurement time of the calibration.

5.1.2 Central Thimble Flux Calibration

A similar method was used to determine the total neutron flux for the central thimble, but a cadmium covered iron wire was not irradiated to determine the fast flux. The fast flux was determined theoretically using an MCNP model and the specifications provided for the reactor. Irradiating cadmium creates radioactive isotopes that require about one week to decay away before the sample is safe to handle. Due to the long wait time, the cadmium covered iron wire was not irradiated to allow for immediate testing of the MPFD in the central thimble. The central thimble has been well modeled using iron wire calibrations and the thermal to fast ratio is well known. Data for the bare iron wire is provided in Table 5.2 along with the calculations for the thermal and fast flux using a fast to thermal ratio of 1.2 [5].

Table 5.2 The calculated central thimble flux from the flux wire experiment.

Central Thimble Flux Calibration								
Bare Iron Wire								
Wire Seg.	Length (cm)	Mass (mg)	Activity (μCi)	Act. Error (μCi)	Thermal Flux ($n/cm^2 \cdot s$)	Uncertainty ($n/cm^2 \cdot s$)	Fast Flux ($n/cm^2 \cdot s$)	Uncertainty ($n/cm^2 \cdot s$)
1	1.27	4.9	6.917E-02	1.92E-03	1.023E+13	2.89E+11	1.228E+13	3.47E+11
2	1.27	5.0	7.716E-02	2.12E-03	1.118E+13	3.12E+11	1.342E+13	3.74E+11
3	1.27	5.1	7.979E-02	2.19E-03	1.134E+13	3.16E+11	1.361E+13	3.79E+11
4	1.27	5.1	8.180E-02	2.23E-03	1.162E+13	3.23E+11	1.394E+13	3.88E+11
5	1.27	4.9	7.971E-02	2.18E-03	1.179E+13	3.28E+11	1.415E+13	3.94E+11
6	1.27	4.8	7.970E-02	2.18E-03	1.203E+13	3.35E+11	1.444E+13	4.02E+11
7	1.27	5.1	8.613E-02	2.35E-03	1.224E+13	3.39E+11	1.469E+13	4.07E+11
8	1.27	5.0	8.254E-02	2.25E-03	1.196E+13	3.32E+11	1.435E+13	3.98E+11

Thermal flux calculations in Table 5.2 match the expected order of magnitude for the central thimble flux [5]. The first wire segment represents the flux at the bottom of the central thimble. At the 7^{th} wire segment the wire is located 2 inches above the center of the core and has the highest flux in the reactor core. This is the preferred location for testing the MPFDs and has

a thermal flux of 6.12×10^7 n/cm^2·s·W. As explained in the IRIS flux calculations section, the uncertainty of the calculated flux in Table 5.2 will have an average 2% of error. The fast flux provided in the table is estimated to have the same uncertainty as the thermal flux multiplied by the fast to thermal neutron ratio (1.2).

5.2 Detection Apparatus

Testing the MPFDs for neutron sensitivity requires equipment that can measure the small current fluctuations from the energy deposited in the fission chamber. Regardless of the type of equipment used, there will need to be at least two sets for measuring detectors simultaneously and replacements for troubleshooting noise issues. Two types of detection equipment are used for testing the MPFDs and both are discussed below. The first is nuclear instrumentation modules (NIM) commonly used for testing detectors and an equipment standard used throughout the world. Fully-integrated circuit boards are the second type of detection equipment and function similar to the NIM equipment.

5.2.1 NIM-bin Setup

The MPFD arrays used for in-core testing were attached to nuclear instrumentation modules (NIM) for use in an equipment bin holder. NIM-bin equipment provides an easy method for testing detectors and troubleshooting problems. Figure 5.1 shows the NIM-bin components configuration used for testing the arrays. Both in-core locations use the same equipment and require the use of all of the equipment to utilize just one device. To operate more than one detector at the same time, the equipment shown in Figure 5.1 will need to be provided for each detector. There are two types of connectors that are attached to the detector arrays. BNC connectors are primarily used with an SHV adapter to connect to the preamplifier (see Figure 5.1). The BNC connectors are easy to attach and require only a coaxial cable to connect

to the NIM-bin equipment. This simplifies troubleshooting the noise and examining the neutron pulses from the detector. Finally, electrical solder pins are the second type of connector used for attaching the detector to the preamplifier. Unlike the BNC connectors, the pins must connect through the electrical feed-through shown in Figure 3.13. Connecting the electrical feed-through will require a c-style connector that has five mini BNC cables attached to provide available test ports for the detectors. The BNC connectors can be attached to the preamplifier.

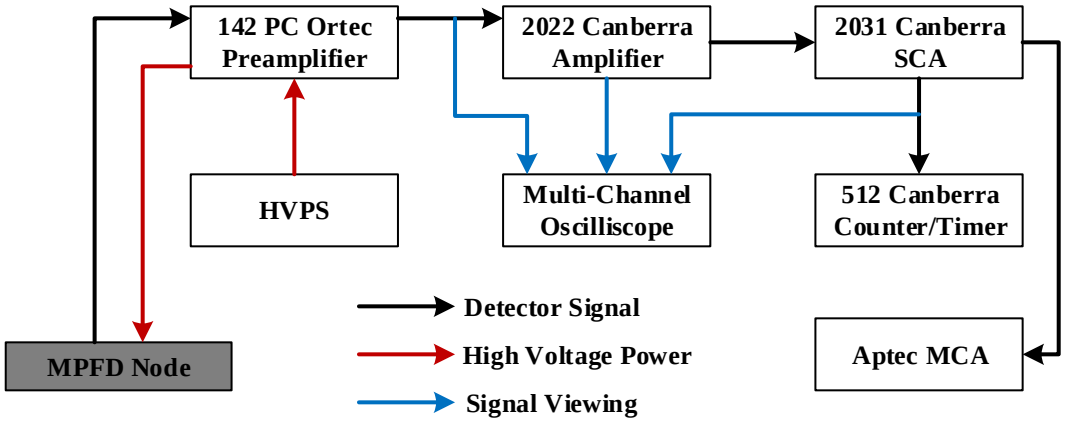

Figure 5.1: Basic setup for a single MPFD node and the detection equipment.

5.2.2 Electronics Board

All the testing conducted for the MPFDs relied on NIM-BIN components is discussed in the previous section. The end goal of the MPFD array is to provide the detectors with integrated electronics that will power the detector, amplify the neutron signal, and display the flux. Every electronic board will operate a single detector and will be housed in a metal box to eliminate noise. An electrical box will contain enough boards to power every detector on the array. Several electronic boards were tested with the MPFDs to determine if the board could process the signal from the detectors. The first electronic board tested was used for analyzing the detector signal from the INL MPFD shown previously in Figure 1.3. Initial testing showed that the detector signal is filtered out from the band pass filter and the electronics are meant to read a signal from the cathode instead of the anode. Attempts were made to modify the existing board

to process the signal, but none of the modifications worked. One other existing board was tested with the array and it was originally meant for lithium foil detectors produced in the S.M.A.R.T. Laboratory. The lithium foil board has similar electronics needed to process, amplify, and measure the signal. A board was tested with the MPFDs and could not develop a signal sent from the chamber. None of the electronic boards worked for the current MPFDs and the results obtained from NIM-bin electronics were sent to Electronics Design Laboratories (EDL) at KSU. Data collected from the future sections will provide EDL with enough information to build electronics board that can process the signal and be used for a final detector package.

5.3 Noise Processing

A single MPFD chamber attached to several feet of wire will behave as an antenna for noise signals entering through the electronic equipment and cables. The signals propagate down the wire and transmit back up causing noise amplification. Amplified noise prevents detection of the signals created from fission events in the MPFD. Locations of the noise can originate from outside radio waves or through the equipment from the power supply. It is important to shield all cables and equipment to prevent unwanted signals from entering and the methods used to shield the detector apparatus are discussed in the sections below. The voltage limitations and detector capacitance are also described in this section to develop an understanding of how the noise is propagated. Finally, the normal detector settings used for detecting neutrons and the common noise level seen while operating the MPFDs will be provided.

5.3.1 Detector Shielding and Grounding

After an MPFD array is attached to the detection equipment in Figure 5.1, the detector signal is analyzed using the oscilloscope to look at the voltage versus time signal from the preamplifier, amplifier, and TTL output from the SCA. Without any shielding or a common

ground, the preamplifier signal shows several volts of noise. Noise is first reduced by shielding every coaxial cable between the detector and the NIM components located in the bin. This includes all of the cables attached to the preamplifier from the high voltage power supply (HVPS), amplifier, and the detector. The best type of shield available for the cable is Inconel over-braid. Inconel over-braid will prevent the signal from entering the detection system when properly grounded. After Inconel over-braid is applied to the coaxial cables, the detector noise on the oscilloscope is reduced to several hundred millivolts. Further reduction of the noise signal is possible by wrapping the preamplifier with aluminum foil to prevent outside signal interference. By shielding the preamplifier, the noise of the detector signal is reduced below 100 mV. To reduce the noise further, the ground loops caused by all of separate over-braid shields need to be removed. Ground loops are removed by connecting the cathode (ground) of the detector to the following components: the test port tube, the over-braid shield, the NIM-bin ground, and the high voltage power supply ground. Removal of the ground loop will reduce the detector noise level to around 50 mV. All of the shielding and grounding lowers the average noise level, but this does not include sporadic increases in noise caused by signals transmitted through the HVPS. Electrical plugins will sometimes propagate 60 kHz frequency noise through the HVPS to the detector. To reduce the 60 kHz noise, a battery backup and AC line filter are placed between the electrical plugin and the detector HVPS. This filter will reduce the noise, but it will not eliminate it entirely. The detector noise on the oscilloscope ranges from 10 mV to 30 mV, depending on the elimination of the ground loops. Finally, a band pass filter can be used to reduce the noise below 10 mV. Initial testing showed that neutron pulses have an effective frequency (based on the pulse rise time) between 1 and 3 MHz. A low pass filter should eliminate most of the noise above 5 MHz and the high pass filter will eliminate most of the noise

below 500 kHz. This band pass filter will reduce the neutron pulse signals slightly, but the small loss of signal compared to the maximized loss of the noise is acceptable. After adding a band pass filter, the detector noise can be reduced to as low as 2 mV. Lowering the noise to below 10 mV will allow for the small neutron pulses to be detected. Initial testing shows that the neutron pulses from the preamplifier will have up to 20 mV signals. By lowering the noise below 10 mV, neutron pulses will not be masked by the amplification of the noise.

5.3.2 Voltage Limitations

Eliminating the noise from the detection equipment allowed for further analysis of the noise caused by other events. As a voltage bias is applied to the detector, the noise level will slightly decrease or remain the same. If the voltage bias is increased high enough, the oscilloscope will record large discharge pulses from the detector (see Figure 5.2).

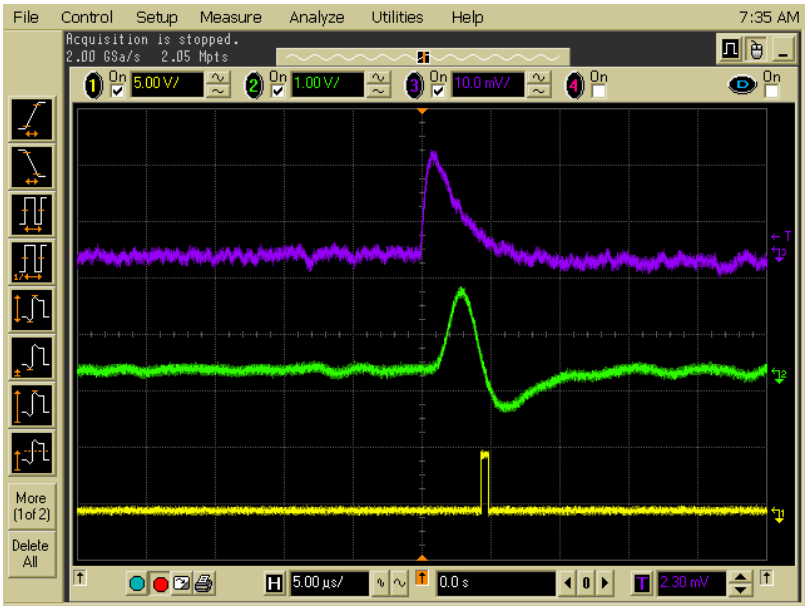

Figure 5.2: Preamplifier (purple), amplifier (green), and TTL (yellow) noise pulse from voltage discharge in the detector chamber.

These discharges are a result of the fissionable material electrodeposited on platinum contacts. The contacts are located between the cathode and anode wire which are only separated by air. When the voltage bias is high enough, the anode wire can discharge to the platinum

substrate causing ionization of the gas medium. Further ionization occurs as the platinum contact discharges to the cathode. Ion pairs created from the discharge will separate and the signal created will have a similar shape to a neutron pulse (see Figure 5.2). Pulses created from the voltage discharge across the fission chamber have characteristics unique to the voltage bias. At a constant voltage bias, all of the discharge pulses will have the same pulse height and occur periodically. The voltage discharges at lower bias will have pulse heights approximately the same height as neutron pulses. Increasing the bias will cause the pulse height of the discharges to increase. MPFD arrays tested for the maximum voltage bias have a limit of 400 V at the HVPS. For the preamplifier used for testing, the voltage bias at the detector is limited to 110 V. The drop in the voltage is due to the preamplifier circuit used to power the detector and amplify the signal from the detector.

5.3.3 Capacitance Measurements

MPFDs use two bare wires in the fission chamber to form a capacitor. When a radiation event occurs, the ion pairs created induce charge flow resulting in measurable current. The capacitance is measured from the detector to the preamplifier. Every preamplifier has a limit on the capacitance input and if exceeded will cause significant noise. For the 142PC preamplifier, the maximum capacitance input is 1000pF. MPFD arrays have a capacitance between 50pF and 80pF. Coaxial cable has approximately 100pF of capacitance for every foot of cable. Therefore, limiting the use of coaxial cable will decrease the noise gain of the preamplifier. Other types of preamplifiers can be used with the low capacitance detector to reduce noise, but the 142PC has a sensitivity of 0.6μV per electron-ion pair. This sensitivity will provide a larger signal for the neutron pulse and is an order of magnitude greater than the other preamplifier models.

5.3.4 Detector Settings and Noise Level

The MPFD arrays used for in-core testing have unique detector settings and noise level that depend on how the array was constructed. However, attempts were made to use similar settings for the detectors. After the detector is inserted into the reactor core and attached to the detection equipment, the voltage bias is set between 300V and 400V depending on the location of the platinum coating in the fission chamber. Next, the amplifier gain is set between 100 and 300 with a shaping time between 0.5μs and 4μs. If oscillatory noise is still present, a higher shaping time will filter the noise out and prevent the TTL from triggering. Finally, the lower level discriminator is raised until the background count rate is 1 or 2 cpm (0.4V to 1.8V). After applying the detector settings, the detector noise level in the IRIS ranges from 10 to 20 mV and the central thimble detectors range from 2 to 5mV. The central thimble detectors are quieter than the IRIS detectors due to the sealed metal tube used for testing.

5.4 Non-Neutron Events

After eliminating the noise in the signal, several non-neutron events are still detected during the measurements. There are several types of random background counts that can occur during the background measurements and are discussed below. Background counts include voltage discharges, large amplified non-bipolar signals, and noise interference. Also, gamma-ray sensitivity of the MPFDs is included to show that MPFDs operate as a fission chambers.

5.4.1 Background Measurements

Before testing neutron sensitivity, background measurements are taken to ensure that the noise level or other non-neutron events do not impede the results. Background measurements are taken after the reactor has been shut down for several hours to prevent detection of delayed neutrons and electronic noise interference. The measurements are first conducted with power to

the console to ensure the noise level does not increase. Other background measurements are acquired with both console power and cooling pumps on. This simulates the normal operating conditions of a nuclear reactor regardless of the power. Low background measurements (< 3 cpm) indicate that the MPFD is ready for further testing. If the background measurements are high, this will indicate that noise pulses from the detector are behaving similarly to neutron pulses. One event that commonly affects such noise is the voltage discharge caused by nickel shavings. As shown in Figure 3.13, nickel shavings from the cathode and anode wires will contaminate the alumina insulator during the assembly process. Nickel shavings will allow for voltage to discharge from the anode to the cathode creating noise pulses that mimic neutron pulses (see Figure 5.3). This problem was understood by applying a voltage across an insulated anode and cathode wire attached to a rough MPFD. Pulses shown in Figure 5.3 were measured and the array was cleaned. Further testing showed reduced noise pulses. Such pulses will occur at a continuous rate depending on the applied voltage and the amount of nickel shaving present. Cleaning the array reduces the chances of measuring the noise pulses caused by the nickel shavings.

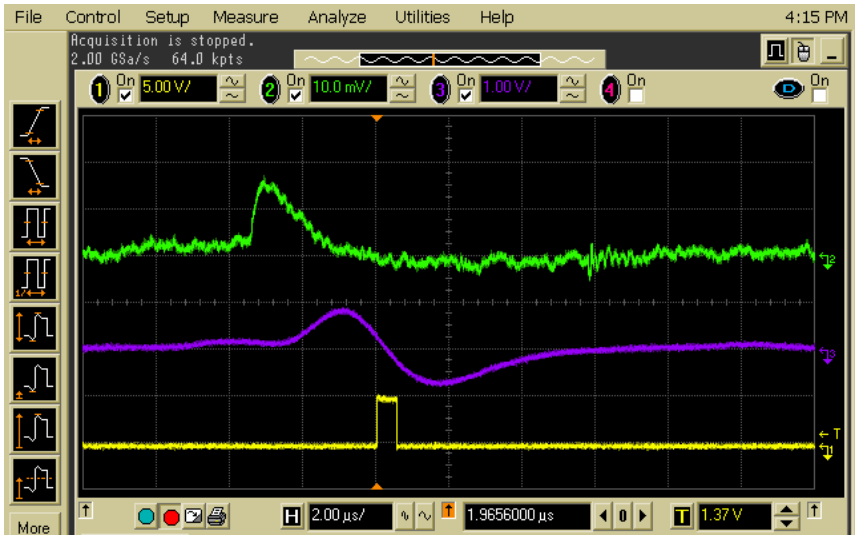

Figure 5.3: Discharges caused by nickel shavings.

5.4.2 Gamma-Ray Sensitivity

An MPFD array was constructed using a rough disk and spacers with no fissile material. This array is used to determine the gamma-ray sensitivity of the MPFD chamber. The chamber size will prevent gamma rays from depositing enough energy to trigger a TTL pulse or provide a visible pulse on the oscilloscope. To demonstrate this effect, the rough MPFD array was placed in the central thimble at the TRIGA Mark II nuclear reactor and tested for a gamma-ray response. The reactor power was at 500 kW to provide a gamma-ray dose of 5×10^4 rad/s. Testing shows that the chamber size prevents measurable energy deposition from gamma rays. Results of the tests conclude that high gamma-ray fields will not deposit enough energy to affect the flux measurements of the fission chamber.

5.5 Neutron Sensitivity

MPFDs are expected to respond linearly to changes in the reactor power by measuring the number of fissions per second (pulse mode) or by measuring the current generated by the fission chamber (current mode) [16, 17]. How the MPFDs respond to changes in the reactor power will determine the operability and limitations of the detectors. In pulse mode, the linear count rate can be modeled to provide the reactor power or the local neutron flux. The detectors must operate in real-time and track changes in the reactor. In-core detectors also need to show a stable count rate for long periods of time and demonstrate that high temperatures of a PWR will not reduce operability. Finally, any flaw that decreases operability will need to be determined to correct the count rate or to remove it from the detector design. The detectors constructed for in-core measurements are tested for the following; dynamic ranges of power, tracking transient power changes, detector stability, and high temperature operability.

5.5.1 Dynamic Range and Transient Testing

Regardless of the location of the detector in the reactor, the first test is dynamic range response to determine the sensitivity of the detector. Dynamic range testing includes identifying the pulses generated from the fission events by using a multi-channel oscilloscope. Shown in Figure 5.4 are common shapes of the neutron pulse from the preamplifier, amplifier, and the TTL output. Neutron pulses can have similar features to the nickel shaving and voltage discharge pulses. Ionization in the fission chamber occurs from all three events and can cause similar pulses. However, background measurements and signal analysis are performed when the reactor is shut down to identify non-neutron events. Average rise times of the neutron pulses are 250 ns and the average fall time is 1.5 µs. Rise times are used to adjust the band-pass filters to further reduce the noise signal and increase detector signals. Average heights of the preamplifier signals are 15 mV and the amplified signal is 1 V (see Figure 5.4). These pulses trigger a TTL output that can be used for multichannel scalers (MCS) or a counter/timer.

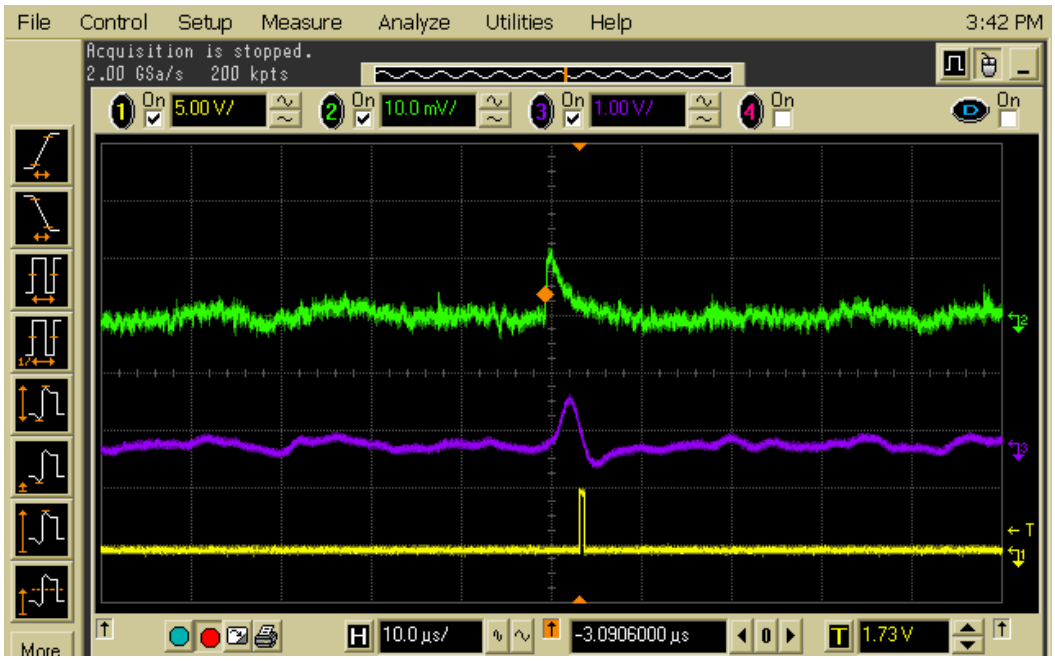

Figure 5.4: Preamplifier (green), amplifier (purple), and TTL (yellow) signal of a neutron pulse from the MPFD.

After collecting the neutron pulse height data, the detectors were tested for linear responses to incremental changes in the reactor power. The power is taken to a constant power level and held within 0.5% of the desired power level. At each power level, a ten minute measurement is taken three times in the IRIS to provide an average of the total counts over a ten minute period. Central thimble measurements were taken five times at one minute intervals. All total counts at various power levels are plotted on a semi log plot as shown in Figure 5.5. Dynamic range plots from detectors in the central thimble and IRIS show a linear response to changes in reactor power. A linear equation was fit to the data using least squares fit to demonstrate the expected response of the detector and the variation from linear operations. The neutron flux in the IRIS is two orders of magnitude lower than the central thimble and requires 10 minute measurements. Despite the low count rate, the IRIS MPFD arrays show sensitivity at 30kW (3.7×10^{10} n/cm^2·s) and linearly track power within two standard deviations of the total counts (see Figure 5.5). Dynamic range measurements for the central thimble were one minute due to the high count rates. Unlike the MPFDs in the IRIS, the central thimble detectors did not track power within two standard deviations of the count rate. This was likely caused by the repositioned control rods to hold power above the point of adding heat. The effect is referred to as control rod shadowing and needs to be investigated further. However, the MPFDs did linearly track the reactor power changes with minimal fluctuation in the count rate at each power level.

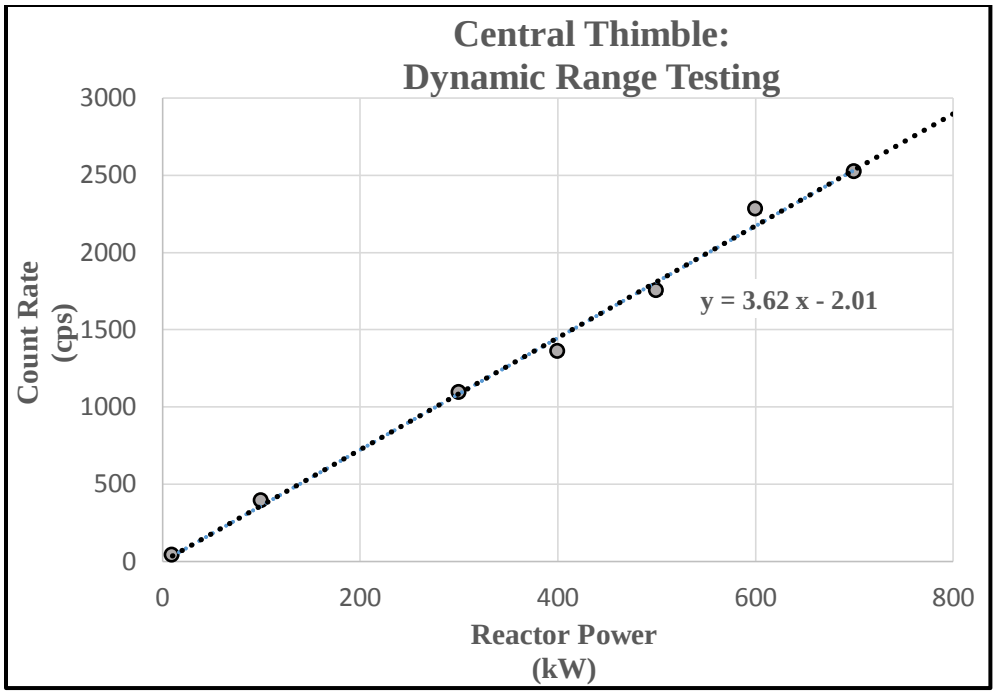

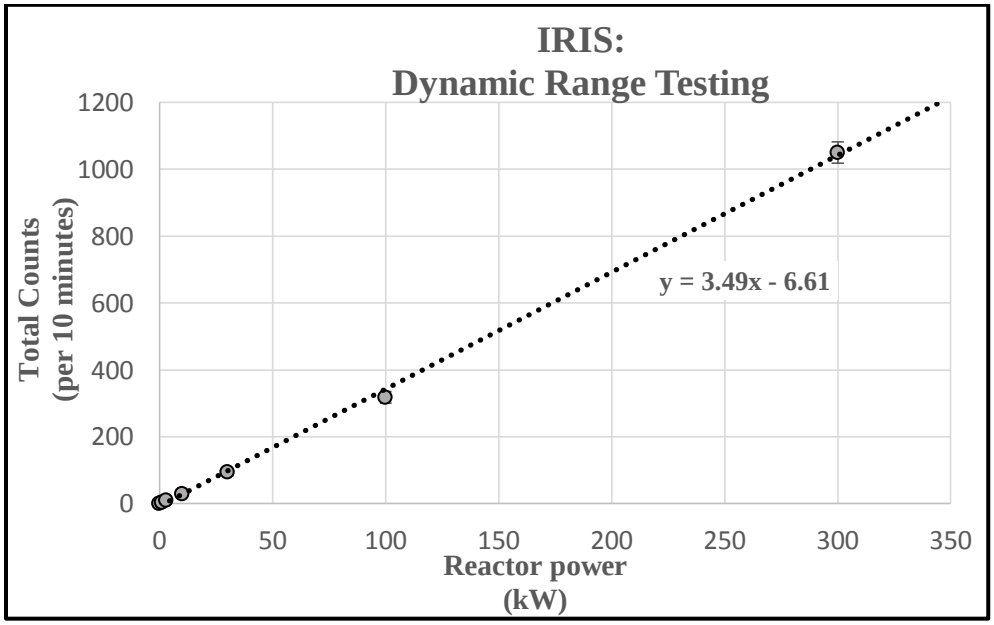

Figure 5.5: The dynamic range testing of a MPFD array in the central thimble (top) and IRIS (bottom).

If the MPFD array responds linearly to the reactor power, the detectors are tested for transient changes in reactor power using a MCS. Transient testing will determine how well MPFDs can track reactivity changes of the reactor. The testing uses positive reactivity insertion of 40, 20, and 10s reactor periods for incremental changes in the power. Also, the testing

includes negative reactivity insertions using \$0.20, \$0.40, and \$0.80 for various shut down speeds. Finally, the reactor will scram to shut down with the fastest negative period of -80s [5]. Shown in Figure 5.6 are the results of an MPFD in the central thimble for transient increases and decreases. During the increasing transient MCS measurement, reactor power is held at 1 kW before and after every reactivity insertion. As shown in Figure 5.6, the three reactivity insertions have an increasing overshoot as the reactor period increases. This overshoot is a result of the reactor power increasing until the fuel temperature heats up, thereby, causing a negative reactivity which causes the reactor to level out at a lower power. A similar response is found with the transient decreasing data (see Figure 5.6). As the reactor power increases, the reactor operator fully removes a control rod and must log the location. The amount of time taken to log the position allows the temperature of the fuel to decrease the reactor power resulting in a small peak. The graphs in Figure 5.6 have a five second moving average trend line to compensate for the fluctuating count rates. Moving average trend lines provide smoother curves to determine how the MPFD response is changing. For negative transient changes, the trend line displays the unique characteristics of the detector. Also, the negative-transient changes are held at higher powers allowing for more stability in the neutron flux of the detectors. Negative reactivity insertions and the reactor scram show a decrease in the response of the detector immediately after insertion (see Figure 5.6). Before the scram, power was increased to 750 kW, but the power did not stabilize before the scram. Both types of transient testing show that the detectors respond to small reactivity changes and shows potential for tracking power in PWRs. Transient testing for the IRIS location was not included in this report due to the low and fluctuating count rates. Count rates and response of the MPFDs are reduced by the low neutron flux and moderator available in the IRIS.

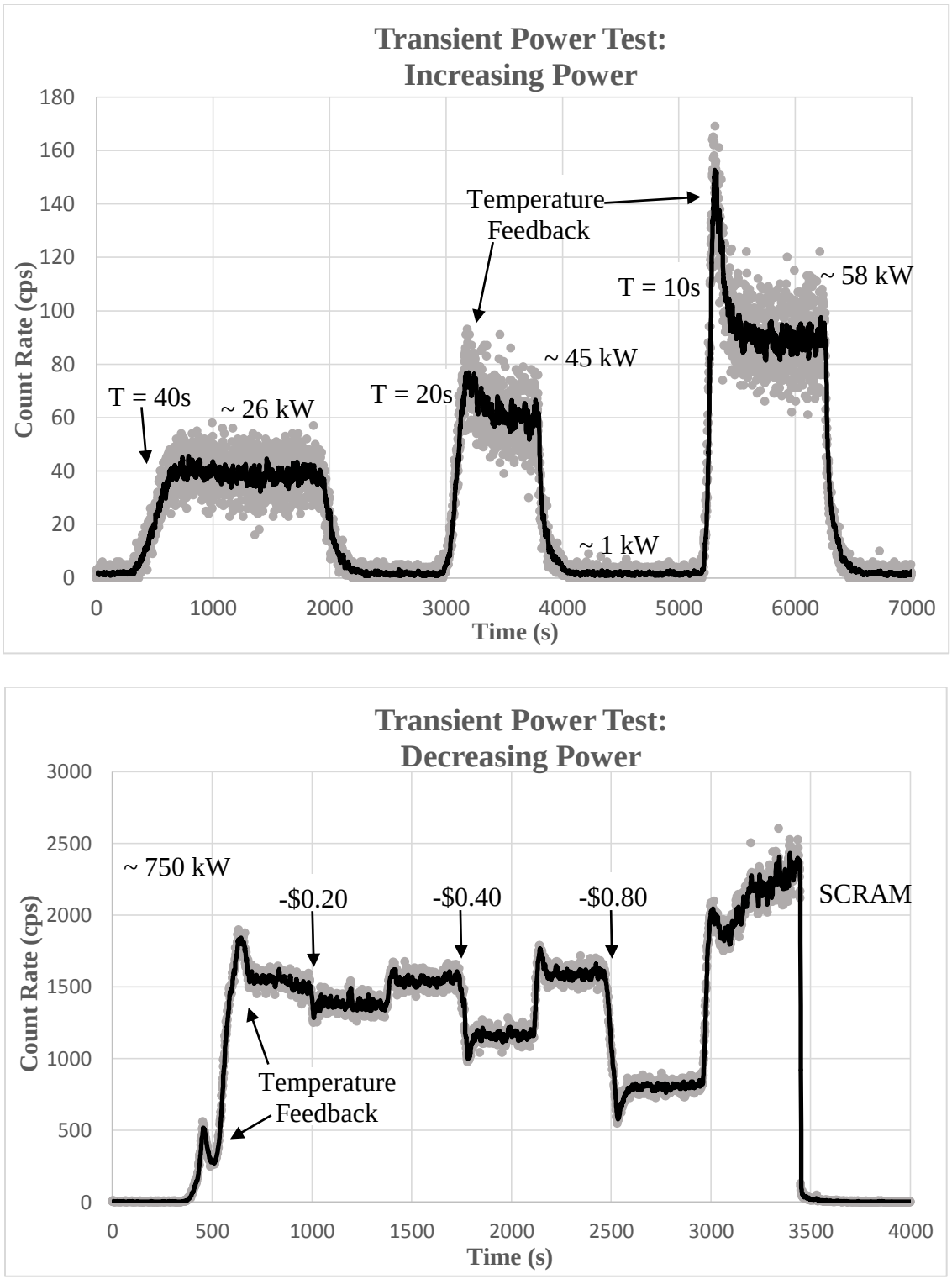

Figure 5.6: Transient increases (top) and decreases (bottom) response results for an MPFD array in the central thimble using a five second moving average for the trend line.

5.5.2 Detector Stability Testing

If the MPFDs show a linear response to the reactor power, the detectors are tested for stability for long term operations. Results from the stability testing of an MPFD determine if the detector chamber can operate consistently without any unforeseen short-term effects. MPFDs in the IRIS are tested for one hour at 300 kW of thermal power. Stability testing determines if changes in the operability of the detector occur over time. If the power fluctuations are less than 2%, the detectors are considered stable and ready for long term operations. The MCS is used for collecting the data and the channel bins are set to one second intervals. A two-node MPFD array was tested at the TRIGA Mark II nuclear reactor in the IRIS. The bottom detector is located one inch from the center of the core and the top detector is two inches from the bottom detector. Also, the MPFD wires were insulated using four-hole insulators for the anodes and the results will provide information for the MPFD cross-talk (see section 5.5.5). Raw data is provided below for the stability testing using total counts collected in five seconds for each bin channel (see Figure 5.7). Included with the measurement data, is a 25 second moving average trend line to show the average neutron flux levels over one hour. As shown in Figure 5.7, the MPFDs consistently measured the neutron flux over one hour of constant testing. The reactor stayed within 0.5% of power and provided detailed information about the MPFD. Large fluctuations in the count rate of the MPFDs are a result of the small mass of the deposited uranium and the limited neutron flux of the IRIS. Also, the MPFDs displayed similar count rates for the stability test despite separate neutron flux locations and different amounts of uranium deposited. The mass of the bottom MPFD used for testing had approximately five times the mass of the top MPFD. Based on the mass alone, the bottom MPFD should provide a count rate five times that of the top MPFD. The similarities in the count rate are discussed further in section 5.5.5.

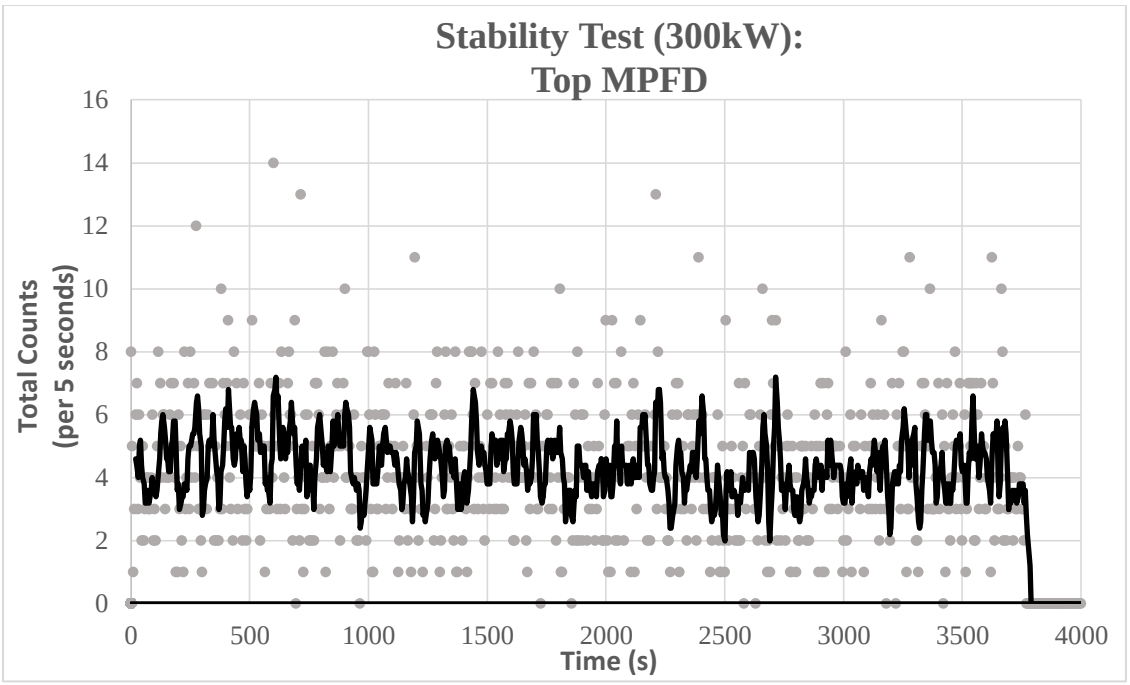

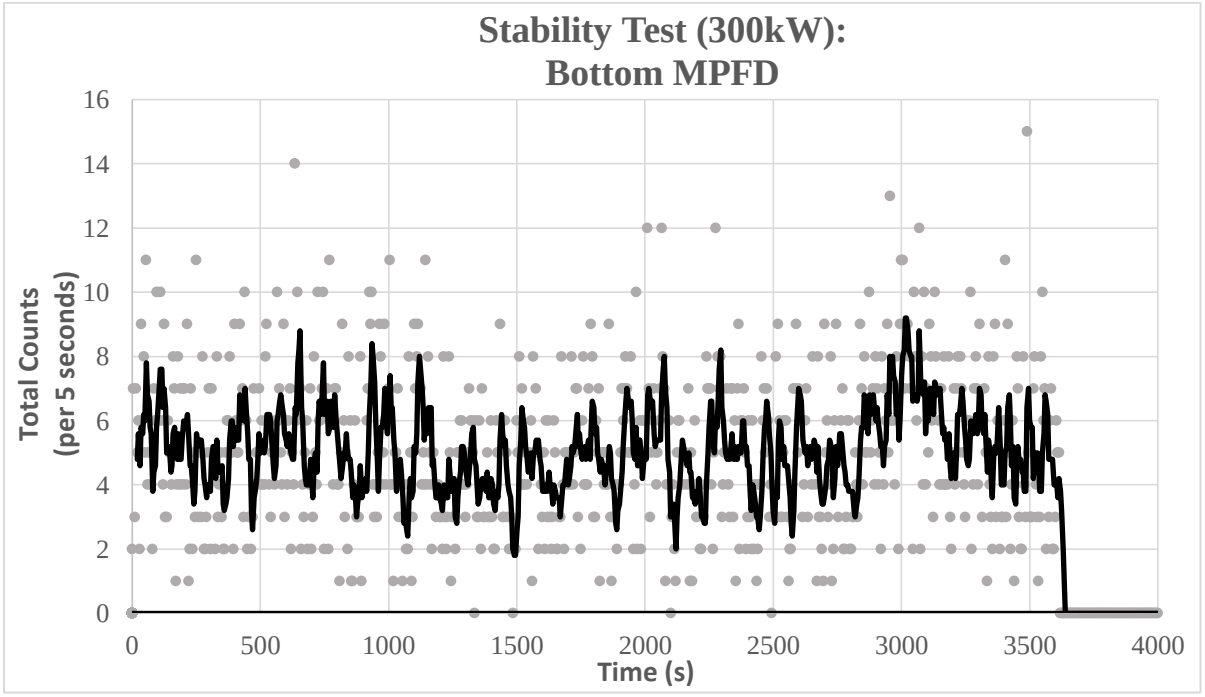

Figure 5.7: (top) The stability results from testing the top node of a two-node MPFD array. (bottom) The stability results from testing the bottom node of the two-node MPFD array.

5.5.3 Response to Reactor Pulsing

Dynamic, transient, and stability testing show that the new MPFD design consistently operates in a high neutron flux and linearly tracks the reactor power. None of these tests caused

more than one percent of dead time for steady state operations. To further test the MPFDs, reactor pulses were performed to test the limitations of the detector response. TRIGA reactors are designed to eject a control rod from the core to increase power a factor by 1×10^8 in less than 10ms. Due to the physics of the reactor, the heat immediately shuts down the reactor and power is reduced below 1 kW in 10ms. Maximum power of the reactor pulse ranges from 400 MW to 1.2 GW depending on the reactivity provided by the control rod ejection. Neutron flux in the central thimble will increase to 10^{17} n/cm^2·s during the pulse and the IRIS location will have 10^{15} n/cm^2·s flux. The higher flux during a reactor pulse will test the dead time of the detector and determine the limiting operability of the MPFDs in pulse mode. Reactor pulse data for the IRIS detectors are located in Figure 5.8-10. A \$1.50, \$2.00, and \$2.50 reactor pulses were used to model the MPFD response (see Figure 5.8 – 5.10).

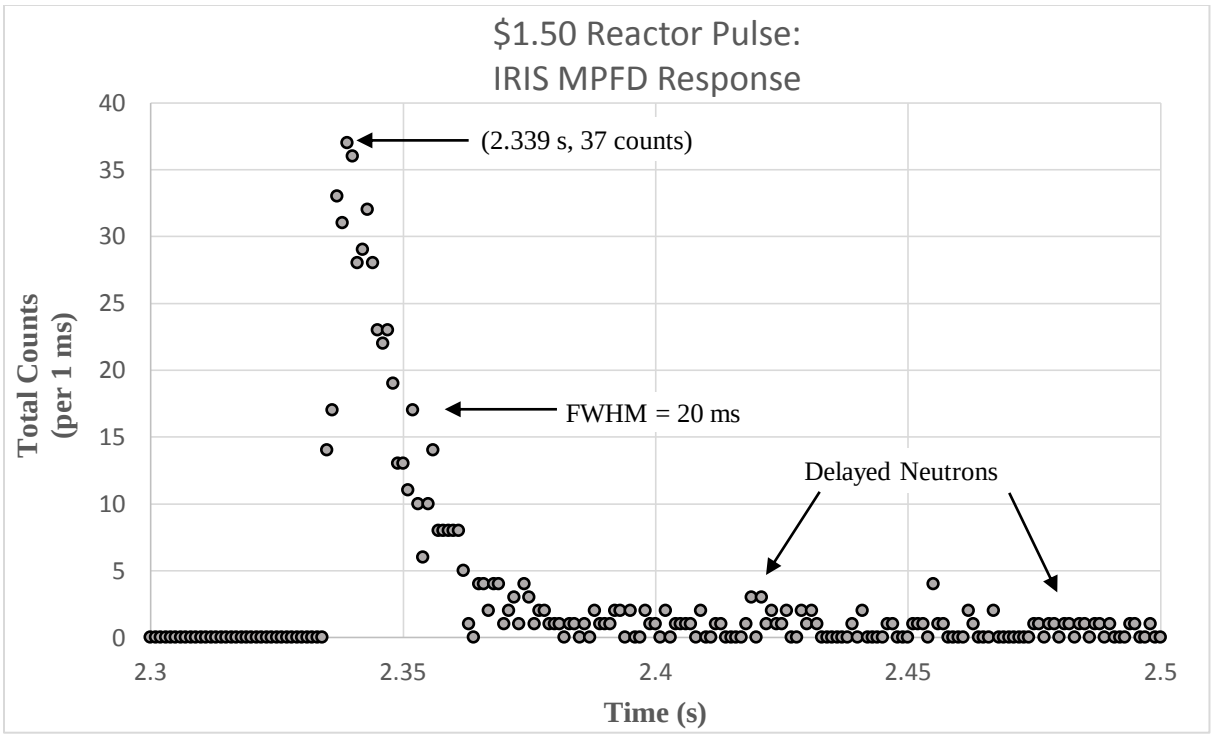

Figure 5.8: Response to a \$1.50 reactor pulse for a two-node detector located in the IRIS.

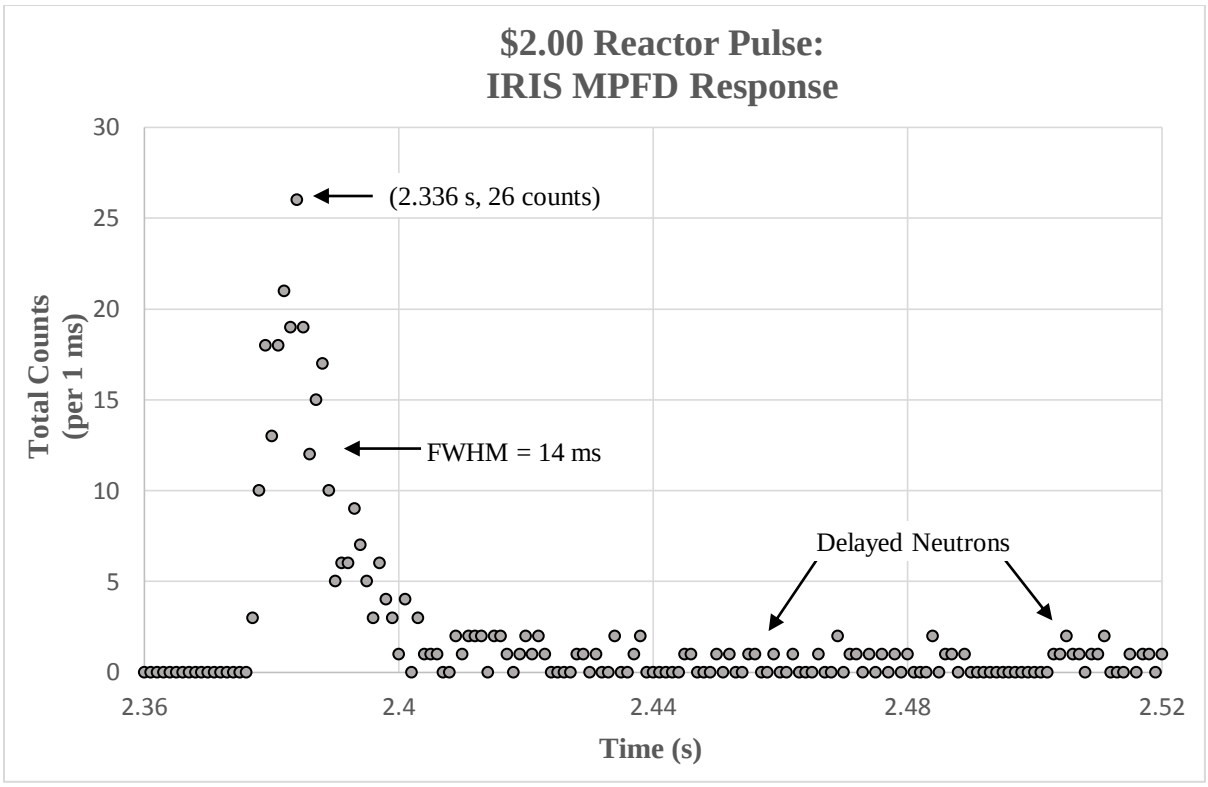

Figure 5.9: Response to a $2.00 reactor pulse for a two-node detector located in the IRIS.

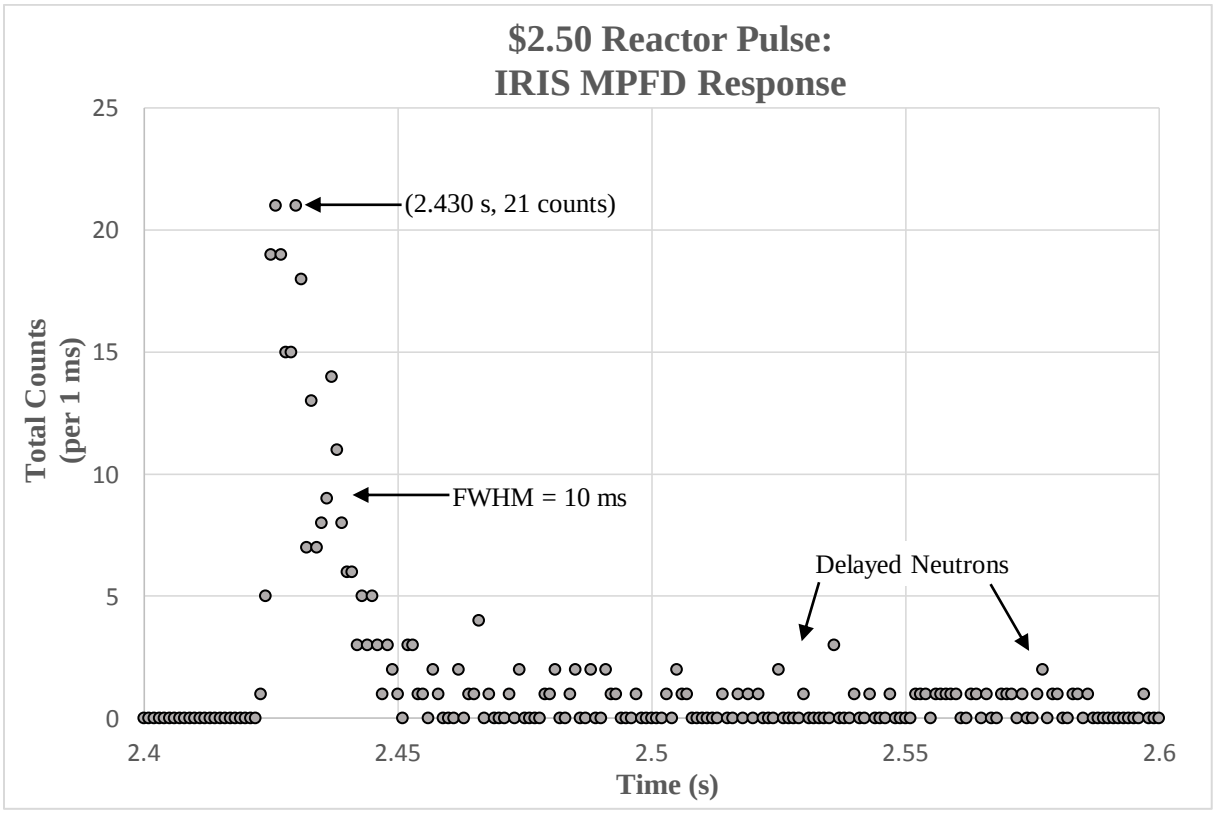

Figure 5.10: Response to a $2.50 reactor pulses for a two-node detector located in the IRIS.

The three measurements in the above figures show that the detector response decreases with an increase in reactivity. This contradicts the expected increase in count rate because of the higher neutron flux achieved from the larger reactivity insertions. However, the increased reactivity decreases the full width half max (FWHM) of the reactor pulse peak. Decreases in the total measured counts suggest that the detector is experiencing significant dead time in the 10^{15} n/cm^2·s flux of the IRIS. To prove that the detectors are experiencing dead time within the IRIS, reactor pulse tests were conducted for the central thimble test port. Reactor pulses in the central thimble should increase the dead time and possibly paralyze the MPFD detectors. The two-node detector used for testing the transient response in the central thimble was used for collecting the reactor pulse data. This MPFD array has one MPFD chamber with fissionable material and one without. Two detector responses for the central thimble were measured for \$1.50 and \$2.00 reactivity reactor pulses (see Figure 5.11). Data from Figure 5.11 shows the total counts collected from the reactor pulses in the central thimble using 0.5 ms bin widths. Unlike the IRIS MPFD results shown in Figure 5.8-10, the measured reactor pulses did not collect the full peak of the reactor pulse. In fact, the detectors did not collect any counts over a period of time depending on the reactivity inserted. This shows that the detectors are paralyzed in neutron fluxes of 10^{17} n/cm^2·s. As the FWHM of the reactor pulse decreases with large reactivity insertions, the time the detector is paralyzed decreases due to the smaller FWHM. Limitations of the detector show that current mode of the detector should be used at flux lower than 10^{15} n/cm^2·s to prevent significant dead time. Also, the MPFD will paralyze in neutron fluxes greater than 10^{17} n/cm^2·s. Dead time and paralyzing flux regions can be changed by controlling the amount of uranium deposited on the MPFD disk.

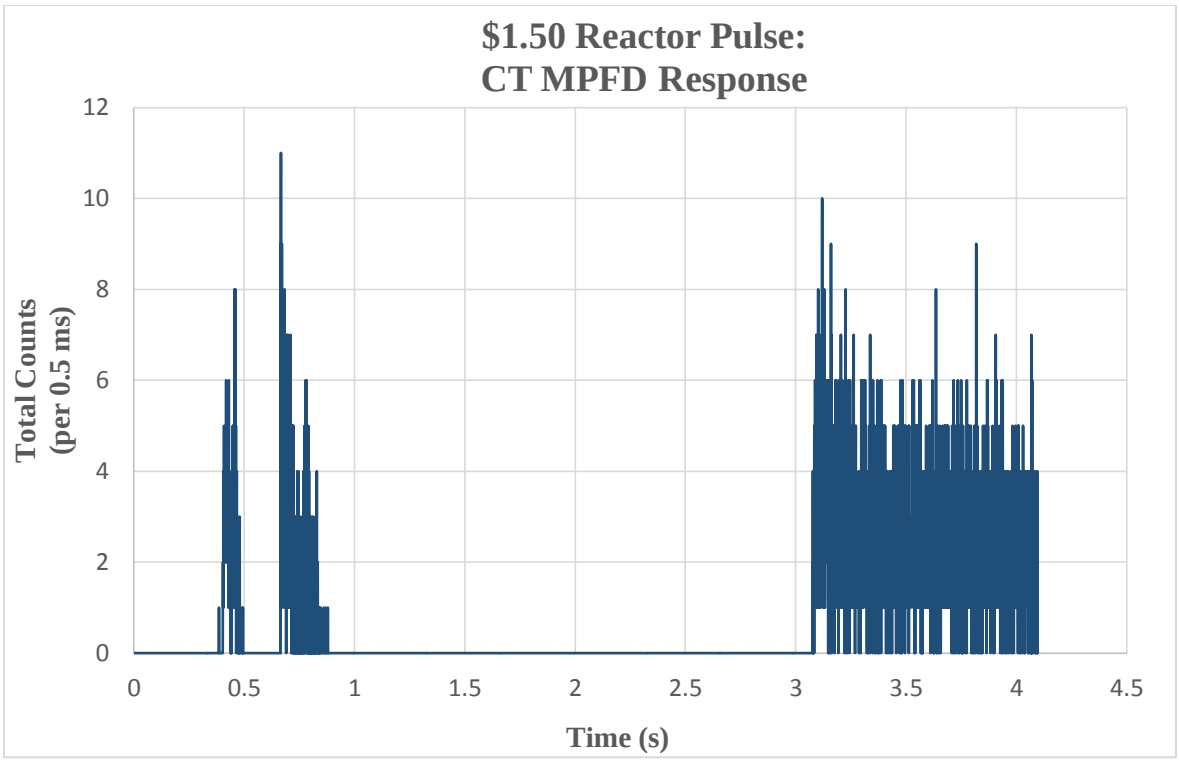

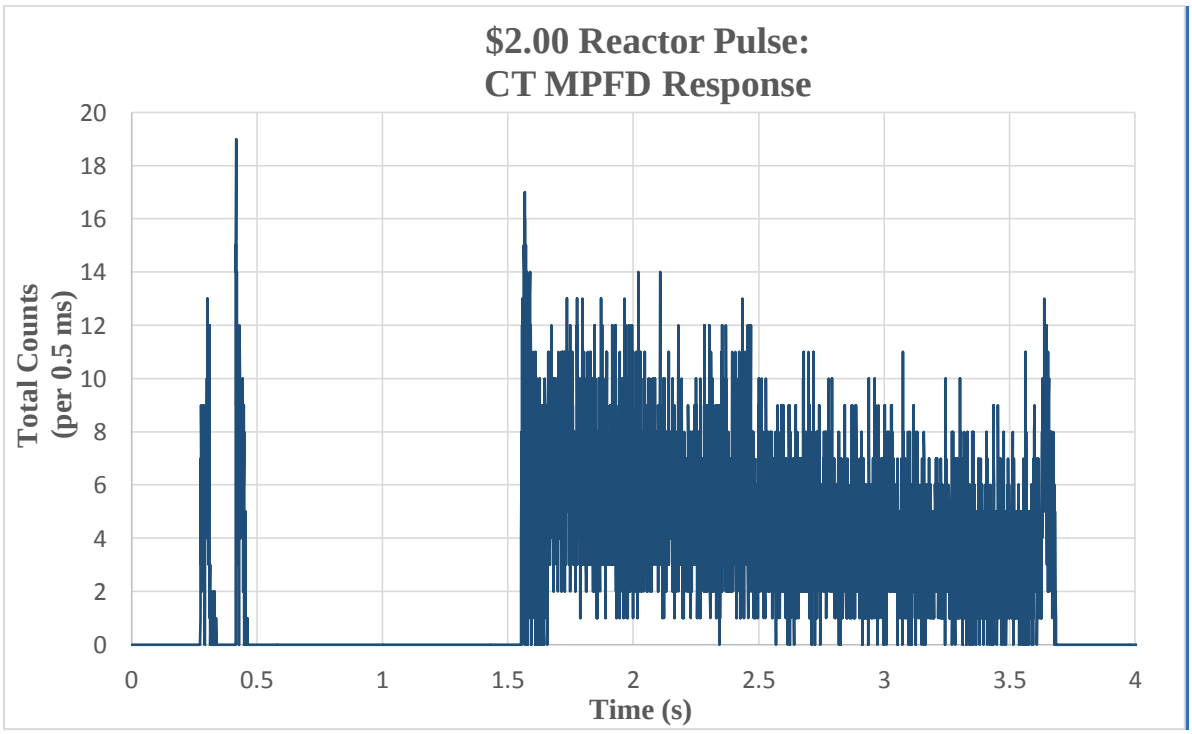

Figure 5.11: Detector response results of a $1.50 (top) and $2.00 (bottom) reactor pulse spectrum collect by a MPFD in the central thimble of TRIGA Mark II nuclear reactor at KSU.

5.5.4 High Temperature Performance

Tests of the MPFDs show that the detectors will operate in high neutron fluxes and that radiation damage does not reduce the performance of the detectors. All of the tests show that these detectors can operate in the high flux regions of PWR for extended operations. However, the temperature in PWRs is higher than the temperatures in a TRIGA reactor. The detectors will have to survive both radiation damage and temperatures up to 600°F. The two-node MPFD array used in the IRIS for stability and reactor pulse testing was removed and heated to 600°F using a three zone furnace at S.M.A.R.T. Laboratories for 24 hours. This MPFD array consisted of two MPFDs and was wrapped with PTFE shrink tube except near the detectors. The high temperature test will determine if the neutron flux causes radiation damage to the MPFD arrays by adding stress on the damage sites. If the detector is still operational after the test, the damage sites in the MPFD array did not cause stress fractures. High temperature and radiation damage were also used to study how the PTFE will behave in a PWR environment. Results of baking the array are shown in Figure 5.12. Alumina for the insulators and MPFD shows no visible stress fractures from the heating of the irradiated material. As expected, the PTFE failed due to the stress caused by the high temperature and radiation damage. In Figure 5.12, the PTFE shows considerable damage to the PTFE and applying pressure will cause the PTFE to disintegrate. Results show that PTFE should not be used in the high flux regions of a nuclear reactor due to the carbon-fluorine structure of the material. Operability of the baked MPFD array was tested by reinserting it into the same IRIS port of the nuclear reactor and using similar detection settings. Previous settings were not matched exactly, because of the various noise interference and changes in the detector location. Despite the changes, the detector demonstrated a linear response to changes in the reactor power before and after the high temperature test.

Figure 5.12: The post bake of a MPFD array at 600°F after 24 hours and the results of the damage caused by both radiation and high temperatures.

These results show that the detectors will operate in high temperature environments; therefore, MPFDs can operate in a PWR. Failure of the PTFE indicates that the detectors should not have PTFE near the active flux region of the reactor core in order to prevent carbon-fluorine molecules from contaminating the fission chamber over time.

5.5.5 Multi-Node Cross Talk

Stability and transient testing of the two-node MPFD arrays show possible cross-talk of the detectors. Cross talk between detectors occurs by transmitting the neutron pulse signal up the intended wire and simultaneously inducing the neutron pulse onto another detector wire. Types of cross talk include capacitive, inductive, and conductive coupling [36]. Capacitive coupling is the unintended coupling of two wires in close proximity that allows signal transmission on both wires [36]. For the MPFD detectors, capacitive coupling is the likely cause for the cross talk between the MPFD wires. Inductive coupling occurs when a change in current through one wire induces a voltage across another wire through electromagnetic induction [29]. Finally, conductive coupling occurs when a signal is transferred by physical contact with a conductive

medium [36]. Conductive coupling will prevent the MPFDs from working and inductive coupling can occur when using a common anode [16, 17]. The cross talk between multiple detectors was discovered during testing by looking at two preamplifier detector signals (see Figure 5.13).

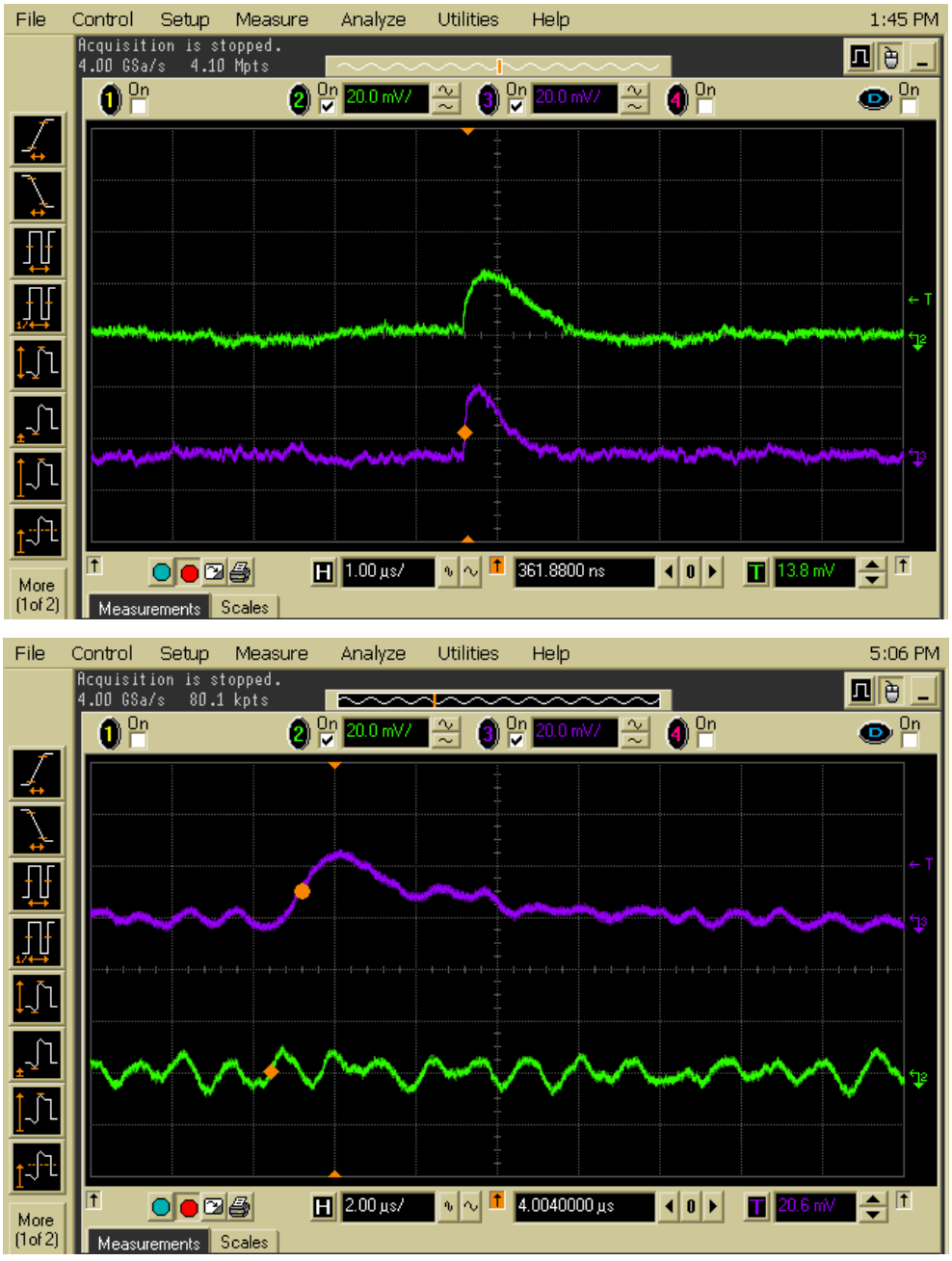

Figure 5.13: (top) The cross-talk from a two-node MPFD array that uses four-hole alumina insulator. (bottom) The prevention of cross-talk using single-hole alumina insulator and PTFE.

Multiple detectors can operate at the same time, but will trigger cross talk counts depending on the proximity of the two anode wires. Tests conducted for a two node MPFD array that uses a four-hole insulator shows that the wires are close enough to cause the cross talk. To eliminate the cross talk, the anode wires need to be separated as far as possible. Single-hole insulators separate the wires far enough to prevent cross talk (see Figure 5.13). This result suggests that the current four-hole insulators do not separate the anode wires far enough to prevent cross talk. However, removing the nickel shavings from the array left small spaces between the insulators showing bare wire. The combined effect of the close proximity of the wires and spaced insulators could cause the cross talk. Single-hole anode insulator is thick enough to prevent the cross talk. The reduction in cross talk of the second MPFD array in Figure 5.13 shows that the coupling is only due to capacitive coupling and not inductive coupling.

Chapter 6 - Conclusions and Future Work

Improvements made to the current MPFD technology were motivated by the desire to provide in-core neutron flux maps of any TRIGA reactor or PWR. Requirements of the detectors include: flexibility and structural integrity for use in flux wire ports, high temperature and radiation damage resistant materials, low neutron activation for easy removal and disposal of the detectors, and long-term measurements of the temperature and neutron flux. The MPFD arrays created to meet these requirements passed the mechanical mock-up and in-core testing. Conclusions and the contributions to the science of in-core neutron detectors are described in this chapter. Finally, future work is considered for improving the MPFD features to simplify the assembly process, increase the neutron sensitivity, and include thermocouples.

6.1 Contributions to In-Core Neutron Detectors

Further development of MPFDs at KSU has successfully produced a new technology for providing multi-dimensional neutron flux measurements in PWRs for long-term analysis of fuel burnup and neutron flux mapping. Testing the mechanical properties and neutron sensitivity of MPFD arrays was successful and it provided a conclusion of what has been accomplished for MPFD assemblies and the detector responses. Previous work on MPFDs did not provide extensive testing of the neutron sensitivity and mechanical properties of the detectors. The testing conducted for the new MPFDs in this report has important implications in the assembly process, detector sensitivity, and noise reduction.

6.1.1 MPFD Assembly

The development and construction of the new MPFD arrays have provided contributions to in-core neutron detector technology. Previous fission chambers are limited by the size of the

detector, location in the reactor, and the number of detectors. Until recently, micro-pocket fission chambers were fragile and used poor construction methods. Current in-core fission chambers use adhesive connections and materials that create long-lived radioactive isotopes from neutron activation. The new MPFD designs developed in this paper have low activation rates and only use mechanical terminations preventing connector failures. Also, the construction materials are flexible enough to allow for the insertion of three MPFDs on an array into a 3 mm diameter metal tube. Available flux wire ports in nuclear reactors have a similar size allowing for the insertion of the MPFDs into new locations previously not accessible. If PTFE is used as a protective sheath, the maximum number of detectors can be increased to five. Materials used for the assembly provide enough structural integrity to survive several insertions and removals into the flux wire ports. These contributions to the MPFD technology improve the arrays' in-core lifetime and allows for long-term operations without perturbations in the flux.

The assembly of the MPFD arrays has provided information for building a working array. Nickel shavings and damaged wires caused by a failed assembly will prevent the detection of neutron pulses. Cleaned MPFD arrays will prevent sporadic voltage discharge pulses that mask real neutron pulses. Mechanical testing shows that MPFD arrays are limited by the coefficient of friction between the alumina insulator and metal tube wall. The difference in Mohs hardness allows alumina to scrape the wall of the tube and cause metal shavings to contaminate the MPFD chamber. Contamination of the array is removed through the assembly process allowing for the collection of neutron pulses. Finally, the materials used for the MPFD arrays demonstrate resistance to radiation damage and have low activation properties to prevent high dose rates during the removal of the detectors. The materials and assembly method used for the new MPFD design provide resilient in-core detectors that can withstand a PWR environment.

6.1.2 Detector Sensitivity

Testing of the MPFDs in the TRIGA Mark II nuclear reactor at KSU demonstrates the capabilities of the detectors as in-core neutron detectors. Results suggest the possibility of MPFD operations within a PWR for long-term applications. Stability testing shows that the detectors withstand the radiation damage and continuously operate. Also, the transient tests demonstrate the MPFD capabilities of tracking changes in reactor power. Tracking of the reactor power can also provide in-core neutron flux measurements. Limitations of the detectors are determined by the reactor pulsing and measuring the response by using an MCS. Implications of the tests show that the detector will experience significant dead time in fluxes greater than 10^{15} n/cm^2·s and paralyze the detector at fluxes greater than 10^{17} n/cm^2·s. Finally, the sensitivity of the MPFDs is limited by the noise and cross talk problems. To increase the efficiency of the detector, both problems must be minimized to allow for the maximum collection of the neutron pulses. To test detectors, the noise reduction of the detector provides an important role in using the MPFDs array. A fission event deposits a large amount of energy, but very little of the signal will make it to the preamplifier. The length of the anode and cathode wires will determine the maximum amplitude of the current pulses making it to the preamplifier. Capacitance and wire resistance determines the size and distance that the pulse can travel. Further reduction in the noise of the MPFD array will allow for better data acquisition and increase the performance. Finally, noise reduction depends on the assembly method of the detector and how well the array is cleaned. As evident from the results, the MPFD provides a new technology that meets all of the requirements of an in-core neutron detector. Improvements over other fission chambers include: access into smaller locations, reduced neutron activation, long-term operations, and multi-node MPFD measurements.

6.2 Future Work

Redesigning the MPFDs has decreased the size of the fission chambers and allowed for successful testing of the detectors in small flux wire ports. Despite the success of this MPFD research, further development will provide data for constructing better arrays, long-term testing, and the adding of thermocouples. The present arrays are unable to utilize the available space for thermocouples and allow for insertion into flux wire ports at the same time. Also, the MPFD array uses cut alumina pieces for insulation and structural integrity. This design may need to be improved to allow for better insertion or prevent noise issues. Finally, the MPFDs developed at KSU have not been tested in a nuclear reactor for long-term use. These three issues are discussed below to provide information on the future work of the current MPFDs.

6.2.1 Thermocouple Designs and Long-Term Testing

Two design requirements were not met for the improved MPFD arrays. First, the MPFD arrays used for successful in-core and mechanical mock-up did not include thermocouples. Adding thermocouples caused all of the arrays inserted into the mock-up to fail due to the friction between the alumina and tube wall. Thermocouple insulator also reduced the flexibility of the array which increased the difficulty of inserting the array into the mock-up. An array that supports thermocouples will have to utilize PTFE shrink tube or use a different type of thermocouple. PTFE will reduce the coefficient of friction and allow for insertion of larger arrays, but it cannot be placed with high neutron flux regions without being damaged. To prevent the PTFE from failing during long-term operations, research will include determining how low the PTFE can be placed on the array to allow for the maximum number of detectors without damaging the PTFE. The other option is to use a new type of thermocouple that could allow for insertion without the use of PTFE. New designs include magnesium oxide insulated

thermocouples with an Inconel 600 metal sheath [37]. Thermocouples diameters of 0.25 mm are available for purchase and can offer structural integrity during the insertion process. The metal sheath is flexible enough to pass through the dogleg of the flux wire port and can allow for the current design to use the new type of thermocouples. The second constraint not met is the long-term testing that will determine the detector limitations from operating in a reactor core and what problems will occur. Final testing will require testing a multi-node MPFD array to determine how the neutron signal changes over long periods of time and what noise issues will occur as radiation damage increases. The long-term testing will also show what isotopes are created from the activation of the detectors and reveal possible solutions on how to further minimize the rate of production. To provide long-term data, a waterproof stainless steel tube is being assembled for in-core testing at flux port M of the TRIGA Mark II nuclear reactor at KSU. Long-term operations at KSUs' nuclear reactor will determine the viability of using the MPFDs in a PWR.

6.2.2 MPFD Array

Several issues are still present in the new MPFD designs. The construction of the MPFD arrays requires expensive materials and extensive time preparing. Analysis of new materials is needed to simplify the construction process and reduce the number of possible problems. The most promising research of furthering the detectors is the use of fused silica capillary tubes. These tubes have smaller diameters to accommodate more detectors and no materials preparation is required. Fused silica is flexible and strong enough to survive the insertion into the mock-up. Possible use of the insulator could increase the maximum number of detectors and prevent cross talk. Replacing the alumina insulator will reduce preparation times, solve cross talk issues, and prevent nickel contamination of the detectors. Initial testing of the silica shows promising results for improving the quality of the MPFD arrays.

References

[1] J. J. Duderstadt, L. J. Hamilton, *Nuclear Reactor Analysis*, New York: Wiley, 1976.

[2] G. F. Knoll, *Radiation Detection and Measurement*, 4th ed., New York: Wiley, 2010.

[3] N. Tsoulfanidis, *Measurement and Detection of Radiation*, 3rd ed. New York: Taylor & Francis Group, 2011.

[4] Centronic, "Radiation Detectors: Fission Chambers," http://www.centronic.co.uk/downloads/Fission_Chambers_General_Info.pdf, [April, 2005].

[5] Kansas State University TRIGA Mark II Nuclear Reactor Facility, *Training Manual*, 2011.

[6] M. H. Tilehnoee and F. Javidkia, "Nuclear Reactors," http://www.intechopen.com/books/nuclear-reactors, [February, 2012].

[7] B. Geslot, F. Berhouet, et al., "Development and Manufacturing of Special Fission Chambers for In-core Measurement Requirements in Nuclear Reactors," IEEE Conference on Advancements in Nuclear Instrumentation Measurement Method and their Applications, http://www.researchgate.net/publication/224153059_Development_and_manufacturing_of_special_fission_chambers_for_incore_measurement_requirements_in_nuclear_reactors, 2009.

[8] Westinghouse, "Westinghouse Technology Systems Manual: Incore Instrumentation System," http://pbadupws.nrc.gov/docs/ML1122/ML11223A264.pdf, [April, 2004].

[9] H. Bock and A. Zeilinger, "Radiographic Examination of Irradiated In-Core Neutron Detectors," Nuclear Instruments and Methods, vol. 129, pp. 147-154, 1975.

[10] Oak Ridge National Laboratory, "Materials Selection for a High Temperature Fission Chamber," https://inlportal.inl.gov/portal/server.pt/document/139426/neet2_5_material_selection_for_a_high-temperature_fission_chamber_(ornl-ltr-2012 -331)_pdf, [August 2012].

[11] T. W. Crane and M. P. Baker, "Neutron Detectors," Nuclear Regulatory Commission, http://www.lanl.gov/orgs/n/n1/panda/00326408.pdf, [March, 1991].

[12] M. F. Ohmes, D. S. McGregor, J. K. Shultis, A.S.M.S. Ahmed, R. Ortiz, R. W. Olsen, "Recent Results and Fabrication of Micro-Pocket Fission Detectors (MPFD)," Proc. SPIE, vol. 6319 (2006) pp. 1P1-1P9.

[13] M. F. Ohmes, A.S.M.S. Ahmed, R. Ortiz, J. K. Shultis, D. S. McGregor, "Micro-Pocket Fission Detectors (MPFD) Performance Charateristics," IEEE Nuclear Science Symposium, San Diego, CA, Oct. 29 – Nov. 3, 2006.

[14] D. S. McGregor, M. F. Ohmes, R. Ortiz, A.S.M.S. Ahmed, J. K. Shultis, "Micro-Pocket Fission Detectors (MPFD) for In-Core Neutron Flux Monitoring," Nuclear Instruments and Methods, A554 (2005) 494-499.

[15] M. F. Ohmes, D. S. McGregor, J. K. Shultis, P. M. Whaley, A.S.M.S. Ahmed, C. C. Bolinger, T. C. Pinsent, "Development of Micro-Pocket Fission Detectors (MPFD) for Near-Core and In-Core Neutron Flux Monitoring," Proc. SPIE, vol. 5198 (2003) 234-242.

[16] M. F. Ohmes, *Micro-pocket fission detector (MPFD) development for the Kansas State University TRIGA Mark-II Nuclear Reactor*, Master's thesis, Kansas State University, Manhattan, 2006.

[17] M. F. Ohmes, *Deployment of a Three-dimensional Array of Micro-Pocket Fission Detector Triads (MPFD^3) for Real-Time, In-core Neutron Flux Measurements in the Kansas State University TRIGA Mark II Nuclear Reactor*, PhD Dissertation, Kansas State University, Manhattan, 2012.

[18] M. A. Reichenberger, T. C. Unruh, P. B. Ugorowski, T. Ito, J. A. Roberts, S. R. Stevenson, D. M. Nichols, D. S. McGregor, "Present Status of Micro-Pocket Fission Detectors (MPFDs) for In-Core Neutron Detection," Annals of Nuclear Engineering (2015), in press.

[19] Accuratus, "Aluminum Oxide, Al_2O_3 Ceramic Properties," http://accuratus.com/alumox.html, [2013].

[20] Westinghouse Electric Corporation, "The Westinghouse Pressurized Water Reactor Nuclear Power Plant," http://www4.ncsu.edu/~doster/NE405/Manuals/PWR_Manual.pdf, [1984].

[21] T. S. Byun and K. Farrell, "Tensile Properties of Inconel 718 after Low Temperature Neutron Irradiation," Journal of Nuclear Materials, vol. 318, pp 292-299, 2003.

[22] F. W. Wiffen, "Response of Inconel 600 to Simulated Fusion Reactor Irradiation," ASTM Special Technical Publication, vol. 683, pp 88-106, 1979.

[23] E. M. Baum, M. C. Ernesti, H. D. Knox, T. R. Miller, A. M. Watson, and S. D. Travis, *Chart of the Nuclides*, 17th ed., New York: Bechtel Marine Propulsion Corporation, 2010.

[24] NNDC, "Interactive Chart of Nuclides," http://www.nndc.bnl.gov/chart/, [2015].

[25] R. L. Norton, *Machine Design: An Integrated Approach*, 4th ed., New Jersey: Pearson, 2011.

[26] Omega, "Introduction to Temperature Measurement," http://www.omega.com/prodinfo/thermocouples.html, [2015].

[27] DUPONT, “Teflon PTFE: Fluoropolymer Resin,” http://www.rjchase.com/ptfe_handbook.pdf, [2013].

[28] Kansas State University TRIGA Mark II Nuclear Reactor Facility, *By-Product Logs*, 2015.

[29] McDanel Advanced Ceramic Solutions, “Available Ceramic Technologies,” http://www.mcdanelceramics.com/, [2015].

[30] M. A. Reichenberger, T. Ito, P. B. Ugorowski, B. W. Montag, S. R. Stevenson, D. M. Nichols, and D. S. McGregor, “Electrodeposition of Uranium and Thorium onto Small Platinum Electrodes,” Journal of Radiation Chemistry and Physics, [2015].

[31] CALCE, and University of Maryland, “Material Hardness,” http://www.calce.umd.edu/TSFA/Hardness_ad_.htm, [2001].

[32] Swagelok, “Parts List,” https://www.swagelok.com/, [2015].

[33] MDC, “Vacuum Products, LLC,” http://www.mdcvacuum.com/MDCMain.aspx, [2015].

[34] EPO-TEK, “Two-part Silver Epoxy,” http://www.epotek.com/site/, [2015].

[35] McMaster-Carr, “Solder Flux, PTFE, and Wire,” http://www.mcmaster.com/, [2015].

[36] A. W. Barr, “Analyzing Crosstalk and Ground Bounce in Multiconductor Systems Using SPICE Circuit Simulations,” http://www.te.com/documentation/whitepapers/pdf/3jot_2.pdf, [2004].

[37] Omega, “Thermocouple Technologies,” http://www.omega.com/pptst/304_INC_MM_CLAD_DUAL.html, [2015].

Appendix A - By-Product Calculations

The dose rates calculations used for analyzing MPFD arrays was developed using the training manual provided for KSUs' TRIGA Mark II nuclear reactor [5]. All of the dose rates depend on the considerations made for the by-product logs and will be provided in this chapter. Also, the equation and derivation used to determine the dose rate is shown below and is limited to the by-product considerations made. Finally, a table is provided to demonstrate how any by-product log is determined for a given sample.

A.1 By-Product Considerations

Dose rate calculations depend on the isotopes created from irradiating a sample. Using the known concentrations of the sample, the mass of each isotope is determined and the energy deposition for the dose can be calculated. Any stable isotope of a given element is referred to as the parent isotope and the radioactive isotope created from neutron activation is the daughter isotope. Several assumptions are made to provide a simple method for calculating the dose rate. First, it is assumed that radioactive isotopes created from neutron irradiation will decay into stable isotopes. For most materials, this assumption is true and the other daughter radioactive isotopes created will emit radiation that does not change the dose rate. The second assumption from the calculations is the overestimation of the dose rate. To account for unexpected isotope production, the sample mass is commonly used as the element mass and the parent isotope mass is the sample mass multiplied by the natural abundance. This method assumes that all of the parent isotope will eventually turn into the daughter isotope. Finally, the by-product calculations assume that no neutron multi-absorptions events take place. If a stable isotope absorbs a neutron, the isotope will not capture another neutron before it decays. The assumption is correct for short irradiation times, but it will diverge as the time increases.

A.2 Dose Rate Equation

Equation A.1 shows the variables used to calculate the dose rate and the units commonly denoted [5]. To calculate the dose rate, the activity (C) is kept in curies, the energy deposited (E) is in MeV, the distance from the source (r) is in feet, and n is the branching ratio of the energies deposited [5]. The correction value (6) is used to account for the units used and convert the answer to Rad/hr [5]. Finally, an example is provided in Table A.1 to show how Eq. A.1 is used to determine the dose rate of a given sample [5].

$$DR(Rad \cdot hr^{-1}) = \frac{6C(Ci)E(MeV)n}{r(ft)^2} \quad \text{(A.1)}$$

Table A.1 Alumina by-product calculation example used to determine the dose rates after a specific time in a nuclear reactor.

Sample: Alumina (Al_2O_3)					
Reactor Power: (kW)	500	Thermal Flux: (n/cm²·s)	2.00E+13	Sample Size: (g)	1.00
Irradiation Time: (s)	3600	Fast Flux: (n/cm²·s)	2.40E+13	Avogadro Constant: (N_A)	6.022E+23
Element: Aluminum					
Parent Isotope: (xxx)	27	Thermal X-Section: (b)	0.230	Initial Activity: (Ci)	9.67E+01
Natural Abundance: (%)	100.00	Resonance Integral: (b)	0.170	Activity (1 Month): (Ci)	0.00E+00
Parent Isotope Mass: (g)	1.00	Decay Constant: (s^{-1})	5.13E-03	Initial Dose Rate: (Rad/hr)	1.75E+03
Daughter Isotope: (xxx)	28	Sum of E*n: (MeV)	3.021	D.R. (1 Month): (Rad/hr)	0.00E+00
Element: Aluminum					
Parent Isotope: (xxx)	18	Thermal X-Section: (b)	1.60E-04	Initial Activity: (Ci)	3.03E-05
Natural Abundance: (%)	0.21	Resonance Integral: (b)	8.10E-04	Activity (1 Month): (Ci)	0.00E+00
Parent Isotope Mass: (g)	2.05E-03	Decay Constant: (s^{-1})	2.58E-02	Initial Dose Rate: (Rad/hr)	4.94E-04
Daughter Isotope: (xxx)	19	Sum of E*n: (MeV)	2.719	D.R. (1 Month): (Rad/hr)	0.00E+00
Dose Rate Totals:		D.R. (Initial): (Rad/hr)	1.75E+03	D.R. (1 Month): (Rad/hr)	0.00E+00

Appendix B - Flux Wire Calculations

The iron wire flux calibrations used for this report were calculated based on information provided below. In this section, the procedures used for irradiating the iron wire and measuring the activity are provided. Also, the derived equations used for calculating the fast and thermal neutron flux are provided.

B.1 Flux Wire Procedures

Iron wire flux calibrations do not provide a real-time measurement of the reactor core, but the measurements provide an accurate representation of the average axial flux in a specific location. The experiment starts by inserting a pure iron wire (99.5%) with a known mass and length into the desired location of the reactor core. After insertion, the reactor is taken to 200 kW and the iron wire is irradiated for one hour. After the reactor is shut down, the sample cools down for one hour to allow for short-lived isotopes to decay. The iron wire is pulled from the core, cut into 0.5 inch pieces, and the mass of each sample is measured. Each piece is placed in a plastic bag and taken to a germanium detector. Each sample is placed on the detector and a pulse height spectrum is collected. Using calibrated spectra from known sources, the isotope peaks in the spectrum are identified and a report is generated that provides the activity of each isotope. The ^{59}Fe peaks are used as the activity of the sample and the errors associated with each measurement is provided in the report. All of the steps provided above are repeated for a cadmium covered iron wire. However, the wait time between irradiating and pulling the sample is increased to two weeks. This allows for the activated cadmium to decay away and prevent high dose rates to the worker. After the activity for both wires is measured, the combined data is used to determine the fast and thermal flux. If both wires are not measured, an MCNP model can be used to determine the fast to thermal ratio as discussed in section 5.1.

B.2 Flux Wire Equation

The data collected above will be used in the final equation below to calculate the fast and thermal flux. To calculate the flux, the activity of a specific radionuclide is determined from Eq. B.1 [5]. It is assumed that an isotope, i' will absorb a neutron to produce a radioactive isotope, i. In Eq. B.1, C_i is the activity, Q_i is the constant production rate, λ_i is the decay constant, and t_o is the irradiation time. The constant production rate is calculated using Eq. B.2 [5].

$$C_i = Q_i(1 - e^{-\lambda_i t_o}) \quad [B.1]$$

$$Q_i = \frac{N_a \rho_{i'}}{A_{i'}} \overline{\sigma_a} \emptyset V \quad [B.2]$$

For Eq. 2, N_a is Avogadro's number, $\rho_{i'}$ is the density of the stable isotope, $A_{i'}$ is the atomic mass, $\overline{\sigma_a}$ is the absorption cross-section, ϕ is the neutron flux, and V is the volume. The equation is inserted into Eq. B.1 and the density multiplied by the volume equals the mass of the isotope in the sample multiplied by the density. Results of the derivations are shown in Eq. B.3.

$$C_i = \frac{N_a m_x \rho_{i'}}{A_{i'}} \overline{\sigma_a} \emptyset (1 - e^{-\lambda_i t_o}) \quad [B.3]$$

The equation above can be adjusted for both thermal and fast flux by changing the absorption cross-section. If the fast flux is desired, the cross-section will become the resonance integral and the flux calculated is the fast flux. Thermal fluxes can be calculated by subtracting the fast flux from the total flux. The two equations below show the final equations for solving the thermal and fast flux. In the equations, RI is the resonance integral, $\emptyset_f$ is the fast flux, and $\emptyset_{th}$ is the thermal flux. Finally, the equations below are not adjusted for the wait and measuring time of the samples due to a 44.5 day half-life of the ^{59}Fe.

$$\emptyset_f = \frac{C_i A_{i'}}{N_a m_x \rho_{i'} RI} (1 - e^{-\lambda_i t_o})^{-1} \quad [B.4]$$

$$\emptyset_{th} = \left[\frac{C_i A_{i'}}{N_a m_x \rho_{i'} (\overline{\sigma_a} + RI)} - \emptyset_f \right] (1 - e^{-\lambda_i t_o}) \quad [B.5]$$